

NASA TECHNICAL
MEMORANDUM

NASA TM X-53419

1965

NASA TM X-53419

RESEARCH ACHIEVEMENTS REVIEW
SERIES NO. 14

GPO PRICE \$ _____

CFSTI PRICE(S) \$ _____

Hard copy (HC) 2.50

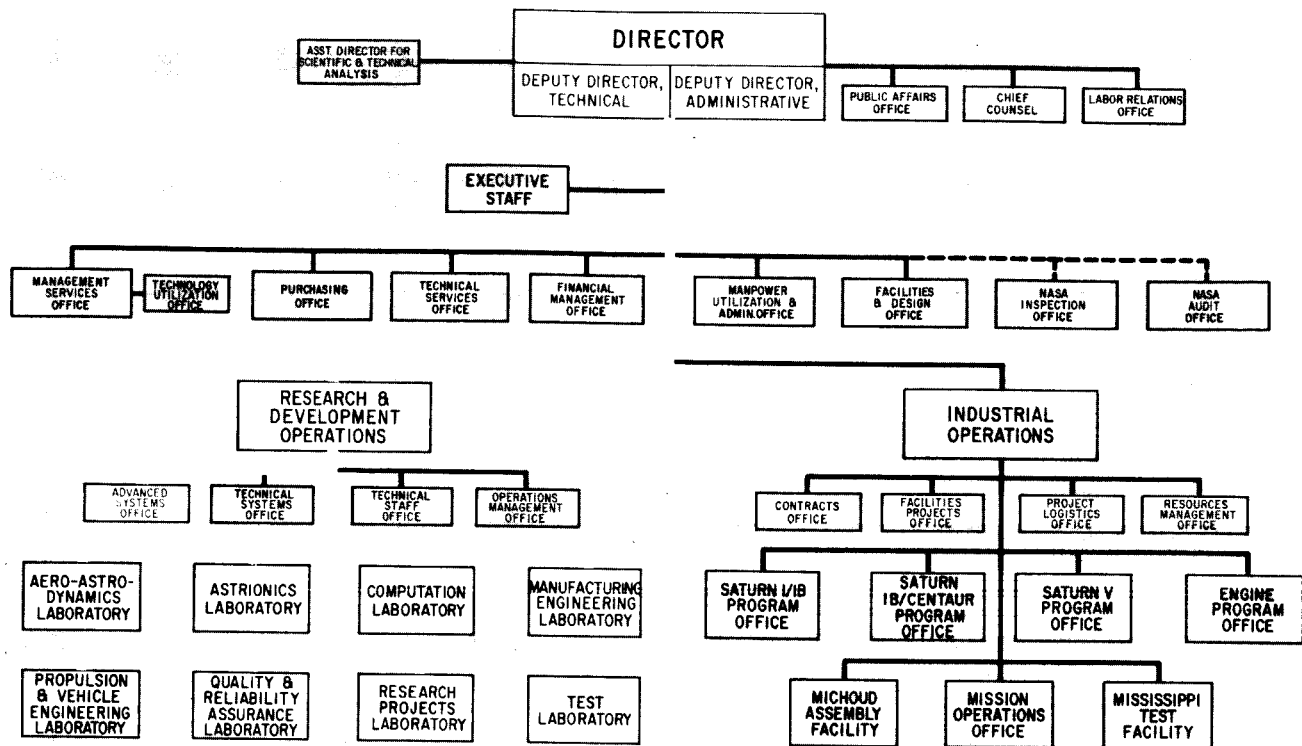
Microfiche (MF) .75

RESEARCH AND DEVELOPMENT OPERATIONS
GEORGE C. MARSHALL SPACE FLIGHT CENTER
HUNTSVILLE, ALABAMA

ff 653 July 65

FACILITY FORM 802	N66 32606	N66 32612
	(ACCESSION NUMBER)	(THRU)
	<u>58</u>	<u>1</u>
	(PAGES)	(CODE)
	<u>TMX-53419</u>	<u>03</u>
	(NASA CR OR TMX OR AD NUMBER)	(CATEGORY)

GEORGE C. MARSHALL SPACE FLIGHT CENTER



RESEARCH ACHIEVEMENTS REVIEW SERIES INCLUDES THE FOLLOWING FIELDS OF RESEARCH

1. Radiation Physics
2. Thermophysics
3. Chemical Propulsion
4. Cryogenic Technology
5. Electronics
6. Control Systems
7. Materials
8. Manufacturing
9. Ground Testing
10. Quality Assurance and Checkout
11. Environmental and Aerodynamics
12. Atmospheric Dynamics
13. Instrumentation
14. Power Systems
15. Guidance Concepts
16. Astrodynamics
17. Advanced Tracking Systems
18. Communication Systems
19. Structures
20. Mathematics and Computation
21. Advanced Propulsion
22. Lunar and Meteoroid Physics

NATIONAL AERONAUTICS AND SPACE ADMINISTRATION
WASHINGTON, D. C.

POWER SYSTEMS RESEARCH AT MSFC

RESEARCH ACHIEVEMENTS REVIEW
SERIES NO. 14

RESEARCH AND DEVELOPMENT OPERATIONS
GEORGE C. MARSHALL SPACE FLIGHT CENTER
HUNTSVILLE, ALABAMA

PREFACE

In 1955, the team which has become the Marshall Space Flight Center (MSFC) began to organize a research program within its various laboratories and offices. The purpose of the program was two-fold: first, to support existing development projects by research studies and second, to prepare future development projects by advancing the state of the art of rockets and space flight. Funding for this program came from the Army, Air Force, and Advanced Research Projects Agency. The effort during the first year was modest and involved relatively few tasks. The communication of results was, therefore, comparatively easy.

Today, more than ten years later, the two-fold purpose of MSFC's research program remains unchanged, although funding now comes from NASA Program Offices. The present yearly effort represents major amounts of money and hundreds of tasks. The greater portion of the money goes to industry and universities for research contracts. However, a substantial research effort is conducted in house at the Marshall Center by all of the laboratories. The communication of the results from this impressive research program has become a serious problem by virtue of its very voluminous technical and scientific content.

The Research Projects Laboratory, which is the group responsible for management of the consolidated research program for the Center, initiated a plan to give better visibility to the achievements of research at Marshall in a form that would be more readily usable by specialists, by systems engineers, and by NASA Program Offices for management purposes.

This plan has taken the form of frequent Research Achievements Reviews, with each review covering one or two fields of research. These verbal reviews are documented in the Research Achievements Review Series.

Ernst Stuhlinger
Director, Research Projects Laboratory

These papers presented September 30, 1965

Page intentionally left blank

TABLE OF CONTENTS

FUEL CELL SYSTEMS

by Richard J. Boehme

	Page
SUMMARY	1
I. INTRODUCTION.	1
II. PROGRAM SUMMARY.	1
III. MANAGEMENT.	2
IV. COMPARISON OF CELL TECHNOLOGY	2
V. UNIQUE FEATURES AND OBJECTIVES	3
VI. PRACTICAL SYSTEMS AND SUBSYSTEMS.	5
VII. SYSTEMS PERFORMANCE	8
VIII. FUTURE PLANS	9

LIST OF TABLES

Table	Title	Page
I.	MISSION REQUIREMENTS VS BREADBOARD TEST RESULTS.	8

LIST OF ILLUSTRATIONS

Figure	Title	Page
1.	Anticipated Range of Fuel Cell Power Requirements.	1
2.	Ion-Exchange Membrane (Acid) Cell.	2
3.	Capillary Matrix (Alkaline) Cell	2
4.	Bacon Cell (Alkaline)	3
5.	Fuel Cell Test Results	4
6.	Fuel Cell Construction Using Static Moisture Removal System	4
7.	Fuel Cell Electrolyte Concentration as a Function of Vapor Pressure and Temperature	4
8.	Cell Construction	5
9.	Closeup View of Typical Assembly	5

LIST OF ILLUSTRATIONS (Concluded)

Figure	Title	Page
10.	Breadboard Assembly Without Outer Canister	6
11.	Sketch of Breadboard Assembly With Outer Canister	6
12.	System Schematic	6
13.	Engineering Model System	7
14.	Special Test Equipment	7
15.	Typical Cell Volt-Ampere Characteristic	7
16.	Results of Breadboard System Test	8
17.	Fuel Cell Output Characteristics	9

TABLE OF CONTENTS

✓ THE DEVELOPMENT OF AN IMPROVED ZINC/SILVER-OXIDE BATTERY

by Charles Graff

	Page
SUMMARY	11
I. INTRODUCTION	11
II. DEVELOPMENT PROGRAMS	11
III. SEPARATOR SYSTEM	11
IV. INITIAL TESTS AND DESIGN GOALS	12
V. EXPERIMENT DESIGN	12
VI. SUMMARY OF RESULTS	13

LIST OF ILLUSTRATIONS

Figure	Title	Page
1.	Typical Discharge Characteristics, Thirty Amperes at 23. 9° C	13

TABLE OF CONTENTS

THE ELECTRICAL POWER SYSTEM FOR THE PEGASUS SATELLITE

by Charles Graff

	Page
SUMMARY	15
I. INTRODUCTION	15
II. EQUIPMENT DESCRIPTION	15
III. BATTERY RECHARGE	16

LIST OF ILLUSTRATIONS

Figure	Title	Page
1.	Block Diagram of Pegasus Power System	15
2.	Maximum Overcharge and Current Allowable for Pegasus Battery	16
3.	Battery Charger Characteristics and Overcharge Limits	16

TABLE OF CONTENTS

BRUSHLESS DC MOTORS

by Dwight Baker

	Page
SUMMARY	17
I. INTRODUCTION	17
II. COMPARISON OF BRUSHLESS DC MOTORS	17
III. COMPARISON OF BRUSHLESS AND CONVENTIONAL DC MOTORS	19
A. Advantages of the Brushless DC Motor	19
B. Disadvantages of the Brushless DC Motor	19
IV. BRUSHLESS DC MOTORS FOR SATURN IB AND V VEHICLES	20
V. PROPOSED BRUSHLESS DC MOTOR APPLICATIONS	20
VI. FUTURE RESEARCH AND DEVELOPMENT REQUIREMENTS	20

LIST OF TABLES

Table	Title	Page
I.	Motor Types and Control Schemes	17

LIST OF ILLUSTRATIONS

Figure	Title	Page
1.	Block Diagram of Inverter Induction Motor	18
2.	Block Diagram of Rotor Sensing Motor.	18
3.	Typical 3 ϕ Output Bridge and Motor Winding	19
4.	Typical Transistor Sequencing and Motor Winding Waveforms	19

TABLE OF CONTENTS

✓ SINGLE-ENDED SWITCHING TRANSFORMER REGULATOR

By Dwight Baker

	Page
SUMMARY	21
LIST OF SYMBOLS.	21
I. INTRODUCTION.	22
II. THEORY OF OPERATION	23
III. OUTPUT FILTER.	26
IV. OUTPUT OVERLOAD PROTECTION	27
V. SINGLE-ENDED SWITCHING TRANSFORMER REGULATOR	27
VI. PRINCIPAL ADVANTAGES	28
VII. FUTURE EFFORTS	28
APPENDIX - DESIGN PROCEDURE.	29

LIST OF ILLUSTRATIONS

Figure	Title	Page
1.	Conventional Method of dc-to-dc Conversion	22
2.	Single-Ended Switching Transformer dc-to-dc Converter	23
3.	Simplified Circuit for Time T_1 Operation	23
4.	Simplified Circuit for Time $T_2 - T_1$ Operation	24
5.	Block Diagram of Single-Ended Switching Transformer dc-to-dc Regulator	27

TABLE OF CONTENTS

ELECTRICAL POWER SYSTEMS STUDIES AT MSFC

by Edward E. Dungan

	Page
SUMMARY	31
I. INTRODUCTION	31
II. INSTRUMENT UNIT RADIOISOTOPE POWER SYSTEM	31
A. Purpose and Objectives	31
B. Status and Schedule	32
C. Program Plans	32
III. LUNAR SURFACE VEHICLE POWER SYSTEM	32
A. MOLAB Fuel Cell Optimization Program	32
B. In-House Computer Program	33
IV. CONCLUSIONS	33
APPENDIX A	34
APPENDIX B	39
APPENDIX C	41
REFERENCES	43

LIST OF TABLES

Table	Title	Page
A-I.	Summary of Daily Power Requirements	35
A-II.	Kilowatt Levels for Profile Variations	36

LIST OF ILLUSTRATIONS

Figure	Title	Page
1.	Power and Energy	32
2.	Fuel Cell Selection and Analysis	33
A-1.	Power Distribution System Functional Interface Block Diagram	37
A-2.	Diode Load Isolation and Buffering	37

N66 32607

FUEL CELL SYSTEMS

By

Richard J. Boehme

SUMMARY

The development of fuel cells at Marshall Space Flight Center is described. Program management and organization are summarized, basic hydrogen/oxygen fuel cell phenomena are reviewed, and developments centered around the asbestos matrix and static moisture removal are described. Practical systems and subsystems are discussed and performance figures are given.

I. INTRODUCTION

Investigation of fuel cell technology and its applicability to space vehicles dates back to 1958 at the Marshall Space Flight Center, which was then known as the Army Ballistic Missile Agency.

Surveys of power requirements for various mission concepts continued to indicate a growing need for fuel cell systems to furnish electrical energy. The range of power requirements for which fuel cells were anticipated is shown roughly in Figure 1. Tradeoff limits are only approximate, but the figure is still considered applicable today. These limits must be

tempered with such factors as availability, complexity, reliability, and cost for any particular application.

The present fuel cell program was initiated in November 1961 when proposals were solicited from 12 sources for research and development work.

The Allis-Chalmers system was selected as the one offering the most advantages for space vehicle application, at least for the next ten years, and a research and development contract was negotiated in May 1962. This work has been sponsored by the Office of Advanced Research and Technology.

II. PROGRAM SUMMARY

The fuel cell program established at the Marshall Space Flight Center is summarized as follows.

1. Major Effort. The major effort is represented by contract NAS8-2696, entitled "Fuel Cell Systems," with the Allis-Chalmers Manufacturing Company. The contract consists of three categories:

- a. Research and Technology Tasks
- b. Breadboard Systems and Laboratory Support
- c. Engineering Model Systems

2. Associated Contract. An associated contract (NAS8-5392) has been in effect since mid-1963 to supplement the program with theoretical studies, mathematical models, and computer analysis of systems and subsystems.

3. In-House Support. The in-house support for the program consists of five types of effort:

- a. Evaluation of Alternates. Components and subsystems.
- b. Preliminary Designs and Breadboards. Advanced electrical controls, converter, and instrumentation.

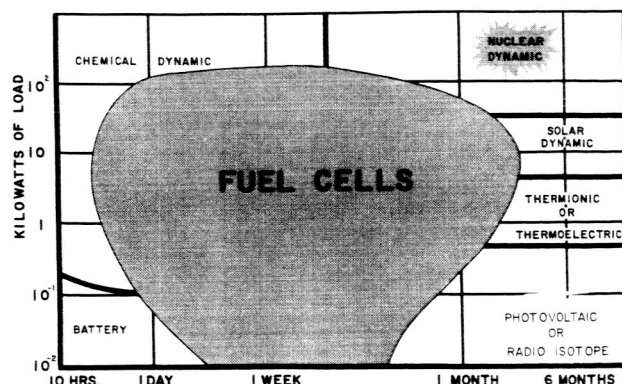


FIGURE 1. ANTICIPATED RANGE OF FUEL CELL POWER REQUIREMENTS

- c. System Studies and Analyses.
Electrical interface, thermal, and vibration.
- d. System Testing and Evaluation.
Performance, environmental, and interference.
- e. Establishment of Guidelines.
Preferred parts lists, fabrication techniques, and specifications.

III. MANAGEMENT

Program management has been quite successful. A small, informal working group of directly concerned personnel from the Office of Advanced Research and Technology, Office of Manned Space Flight, Manned Spacecraft Center, and Marshall Space Flight Center has been established for program planning and coordinated control. This group meets monthly to review the progress and to resolve outstanding problems.

Marshall Space Flight Center has the responsibility for contract administration; however, since August 1964, responsibility for technical supervision is shared by the Manned Spacecraft Center and the Marshall Space Flight Center.

IV. COMPARISON OF CELL TECHNOLOGY

Some of the objectives that have been achieved and the outstanding advantages of the system that has been developed are described in this paper. To establish these advantages, some of the basic fuel cell phenomena that characterize present hydrogen/oxygen fuel cell systems are reviewed.

Figure 2 depicts an early ion exchange membrane cell developed by the General Electric Company. This cell is basically an acid type. The porous electrodes consist of metallic screens embedded in platinum powder bonded to both sides of the exchange membrane. The 0.0254 cm (10-mil) thick polymer membrane represents an acid electrolyte between electrodes. Sulphonic acid was added later to increase the current capacity.

Gaseous hydrogen and oxygen admitted to the cell cavities are absorbed within the electrodes where, in the presence of the catalyst, a complex

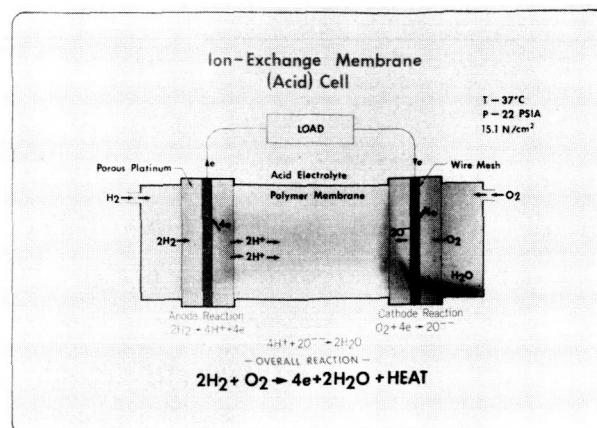


FIGURE 2. ION-EXCHANGE MEMBRANE (ACID) CELL

electrochemical reaction occurs that results in the simplified electrode reactions shown on the illustration. Electrical energy results from the electrons that are released by the ionization of hydrogen.

Transfer of the hydrogen ions through the membrane is accomplished by an electronic diffusion mechanism to a zone at the cathode, where they combine isothermally with the oxygen species to form water. Therefore water must be primarily removed from the oxygen side.

A temperature of 35°C and a pressure of about 15 N/cm² (22 psia) are normally used for this cell.

A basic alkaline cell used in the Allis-Chalmers system is shown in Figure 3. Note that the resultant reactions are similar, but the mechanisms are quite different. Major differences are:

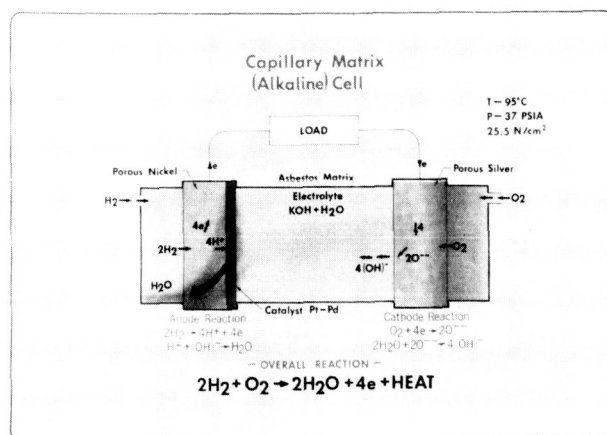


FIGURE 3. CAPILLARY MATRIX (ALKALINE) CELL

1. The electrolyte is a KOH solution held by the high capillary forces of a 0.0508 or 0.0762-cm (20 or 30-mil) -thick asbestos mat.

2. The porous anode consists of nickel sintered on a nickel screen and catalyzed with 4.6 mg/cm² each of platinum and palladium.

3. Allis-Chalmers now uses silver, without catalysts, for the cathode.

4. Electrical conduction within the cell is mainly attributed to hydroxyl (OH) ion transport.

5. Water is inherently formed at the hydrogen electrode and must be removed from that side.

6. Normal pressure and temperature for this cell are 25.5 N/cm² (37 psia) and 95°C, respectively.

The basic Bacon cell is used in the Pratt and Whitney Apollo fuel cell system. The basic reactions are no different from those described for the Allis-Chalmers cell. Notable differences not obvious from the basic diagrams of Figures 3 and 4 are:

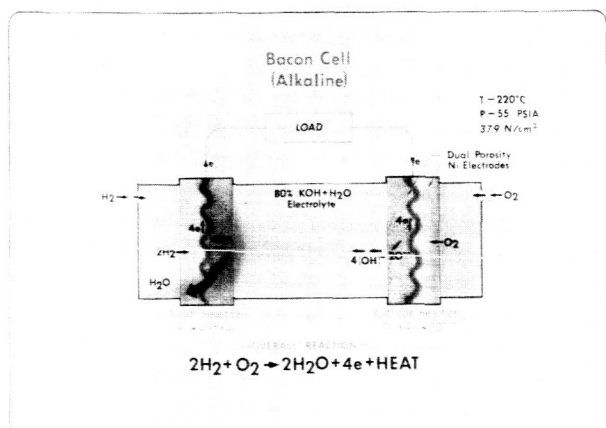


FIGURE 4. BACON CELL (ALKALINE)

1. Dual porosity sintered nickel electrodes are required without catalyst.

2. The KOH concentration of about 80 percent is a solid below 150°C. It must be retained between the porous electrodes.

3. Normal operating conditions are 37.9 N/cm² (55 psia) for pressure and about 220°C for temperature.

Inherent advantages that the Allis-Chalmers system has by virtue of its type and class of cells can be summarized as follows:

1. Alkaline cells inherently offer higher electrical performance, current density, and efficiency than do acid cells; they offer these advantages without the high probability of problems with materials. These advantages are even greater when ion exchange membranes are present, since ion exchange membranes incur higher impedance and are deteriorated by temperatures above 60°C, which limit the allowed chemical activity.

2. Presently, the ion exchange cells produce nonpotable water (pH = 2) and are severely limited in their shelf life and the number of starts.

3. Advantages of the Allis-Chalmers cell over the Bacon cell because of the lower temperature, pressure, and KOH concentration are:

- a. The more rapid degradation mechanisms are avoided, such as crystalline (or dendrite) growth, excessive cathode oxidation, plugging of manifold orifices, and problems with seal materials.
- b. Very long critical startup and shutdown and stresses created by phase change of electrolyte are avoided.
- c. Lower parasitic power is required for standby.

V. UNIQUE FEATURES AND OBJECTIVES

Ruggedness, simplicity, and stability — three of the primary objectives of the Marshall Space Flight Center program — have been met by developments centered around the asbestos matrix and the static moisture removal concept. Simultaneously, outstanding silver electrodes have been developed that have improved electrical performance and life.

Water management is of paramount importance to high performance and successful operation of fuel cells. Water is produced in the cells at a rate directly proportional to the load and must be removed or else the performance will decay as the cells become flooded. If too much moisture is removed, electrolyte drying can decrease performance and increase heating to the point of burnout.

Test results (Fig. 5) have shown that there is an optimum range of KOH concentration in the electro-

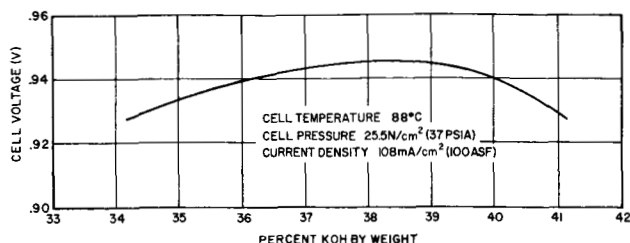


FIGURE 5. FUEL CELL TEST RESULTS

lyte for a given temperature and pressure. For the subject asbestos matrix cells, which operate at about 95°C and 25.5 N/cm² (37 psia), 27 percent KOH and 45 percent KOH have been established as the practical limits of electrolyte concentration for sustained operations. The electrolyte concentration, being dependent on the amount of water present, is controlled by the water removal subsystem based on the unique concept of static moisture removal.

Reference to Figure 6 shows a diagram of a cell cross section where asbestos is used as the electrolyte holder and as the water removal matrix. Mois-

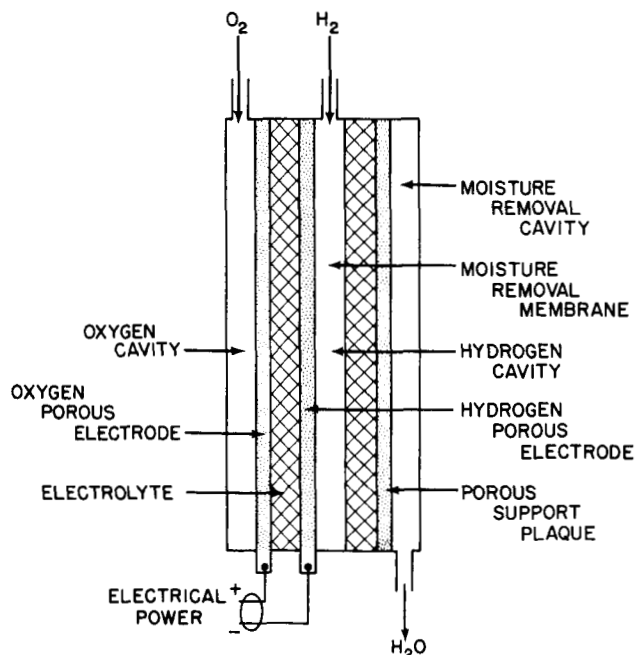


FIGURE 6. FUEL CELL CONSTRUCTION USING STATIC MOISTURE REMOVAL SYSTEM

ture is removed statically and inherently at the proper rate by the moisture removal or transport matrix, which is saturated with a higher concentration KOH solution (say 45 percent) than the 37 percent present in the electrolyte holder. Because of the high capillary force of the asbestos on the KOH, the hydrogen is retained in the hydrogen cavity.

The vapor pressure at a given temperature exerted by each of the membranes will be inversely proportional to its KOH concentration. The vapor pressure of the KOH electrolyte as a function of concentration and temperature is given in Figure 7. The

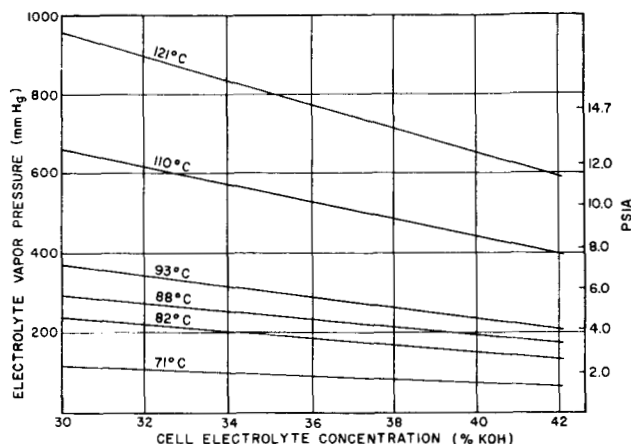


FIGURE 7. FUEL CELL ELECTROLYTE CONCENTRATION AS A FUNCTION OF VAPOR PRESSURE AND TEMPERATURE

water vapor molecules seek equilibrium with the reactant gas molecules, and the sum of the partial pressures of the gases equals the total cell pressure. Now, with the proper pressure setting in the water removal cavity added to the vapor pressure of the water removal matrix, equilibrium can be established for the desired electrolyte concentration.

When product water dilutes the electrolyte, its vapor pressure increases, thereby transferring moisture to the reactant gas. The water removal membrane, having a lower vapor pressure will absorb this moisture to establish partial pressure equilibrium. If the pressure of the water removal cavity is held constant, moisture will be delivered as vapor to the removal cavity by virtue of the increased vapor pressure of the removal matrix.

This concept can be compared to the Apollo fuel cell system which uses a recirculating hydrogen loop

where moisture is removed by circulating excess hydrogen through the cells. Water is then condensed and separated with a centrifugal separator.

VI. PRACTICAL SYSTEMS AND SUBSYSTEMS

The major module developed has been the "fuel cell module" (or stack) which is constructed from standardized cell components. The rugged construction of a single cell, having an electrode area of 372 cm^2 (0.4 ft^2), is illustrated in Figure 8. Plated magnesium plates give structural rigidity, provide the reactant and water removal cavities, serve as current

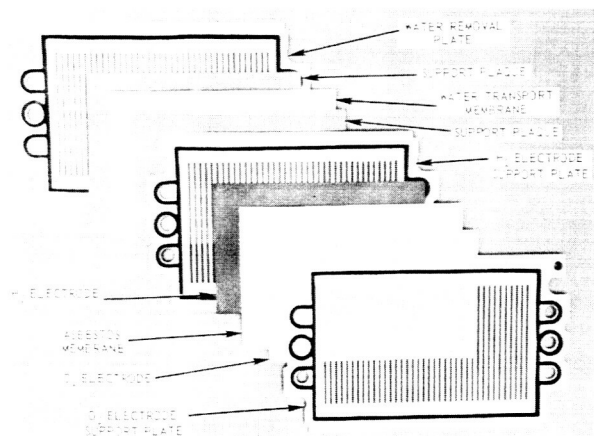


FIGURE 8. CELL CONSTRUCTION

collectors for external connections, and efficiently transfer heat out of the cell. The anode plates are electrodeless nickel plated and the cathode plates are plated with gold over nickel. Note the cell seals, which are rubber O-ring gaskets, and the holes, which form an internal manifolding system when the cells are assembled into a stack. The support plaques are porous metal mats (similar to the electrodes) which evenly support the asbestos and keep it from being compressed into the cell cavities furnished by the manifold grooves in the plates.

The cells are assembled in parallel pairs and arranged so that one water removal cavity serves two cells, conserving weight and space. A closeup view of a typical assembly is shown in Figure 9. Here the intercell connection blocks, some instrumentation leads, and some of the rods which keep several tons of compression on the stack can be seen. The plate fins, which transfer cell heat to a circulating gas

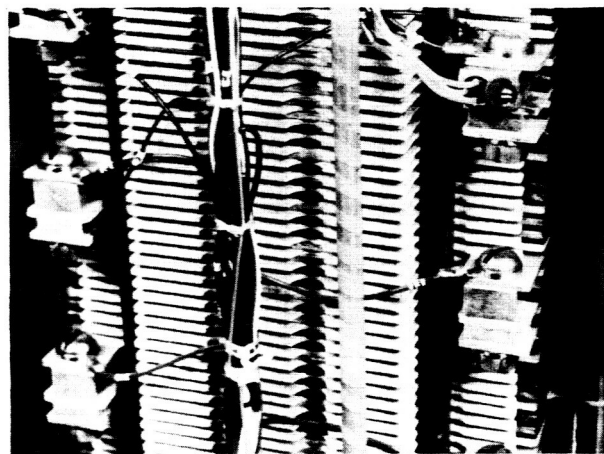


FIGURE 9. CLOSEUP VIEW OF TYPICAL ASSEMBLY

cooling system, are shown protruding beyond the fiberglass spacers to form slots for gas passages along the outer edges of the stack.

A breadboard assembly, without the outer canister, is shown in Figure 10 to demonstrate its rugged simplicity. The fiberglass ducts direct helium coolant gas from two blowers down over the cell fins. The return path is through the intercell slots to the canister and back through a heat exchanger on top of the stack. This is shown better in Figure 11, which diagrammatically depicts the secondary coolant system.

The modular design concept that has been followed throughout, together with the secondary coolant system, accomplishes the objective of versatility; with minimum design impact, this fuel cell system can be interfaced with just about any vehicle liquid cooling system. Neither the Apollo nor the Gemini system has such a feature. Each uses coolant tubes attached directly to each of the cells.

An overall system schematic is given in Figure 12; some of the subsystem features are as follows.

1. Inlet pressure regulators maintain balanced reactant pressures for optimum performance. Pressure differential is far less critical to this system than for the Apollo or Gemini systems because of the rugged cells and the high capillary force of asbestos.

2. The temperature-compensated vacuum-regulator control effects the proper water removal pressure and extends the allowable operating temperature range for startup purposes.

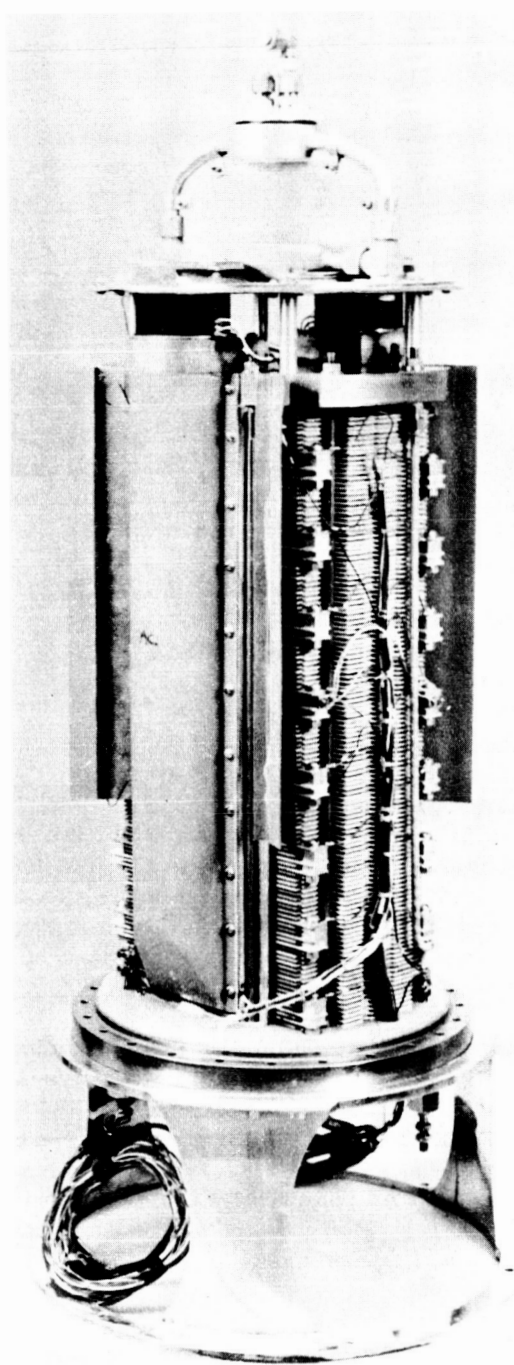


FIGURE 10. BREADBOARD ASSEMBLY WITHOUT OUTER CANISTER

3. The ampere-hour controller assures efficient minimum purging of inerts and impurities that build up in the reactant cavities. With a reactant purity of 99.9 percent, purging requires about 3 percent of the reactant consumed.

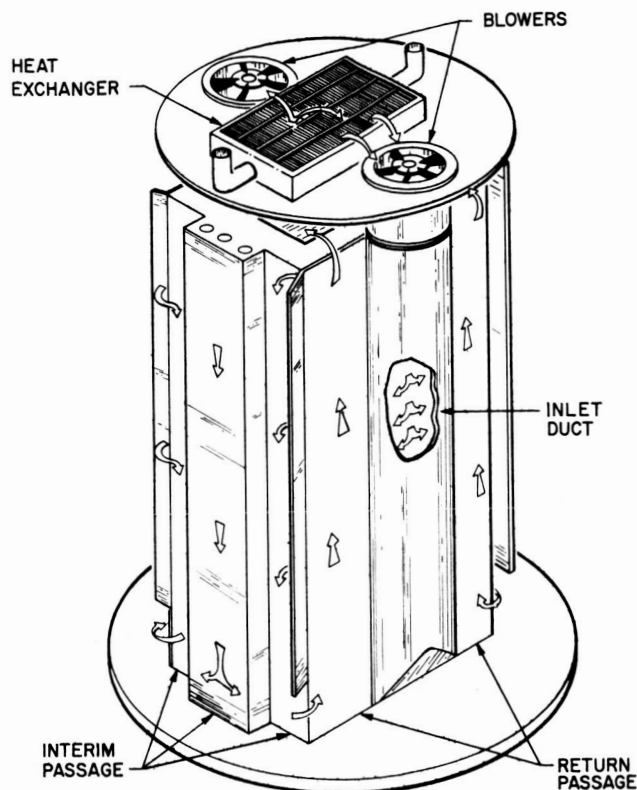


FIGURE 11. SKETCH OF BREADBOARD ASSEMBLY WITH OUTER CANISTER

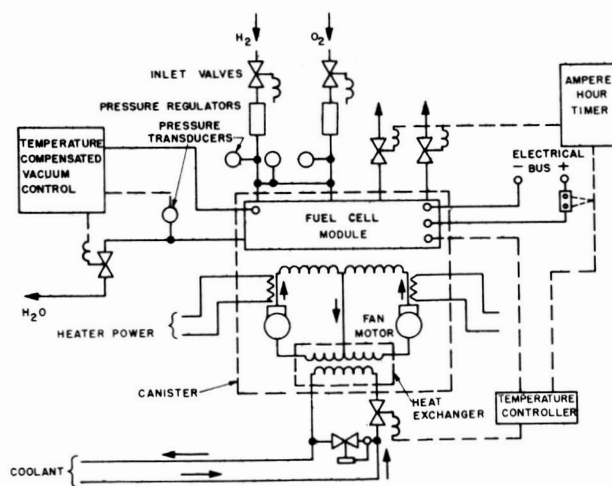


FIGURE 12. SYSTEM SCHEMATIC

4. The heater provides warmup in less than an hour for cold starts.

A complete engineering model system recently delivered to Marshall Space Flight Center for test and evaluation is illustrated by Figure 13.

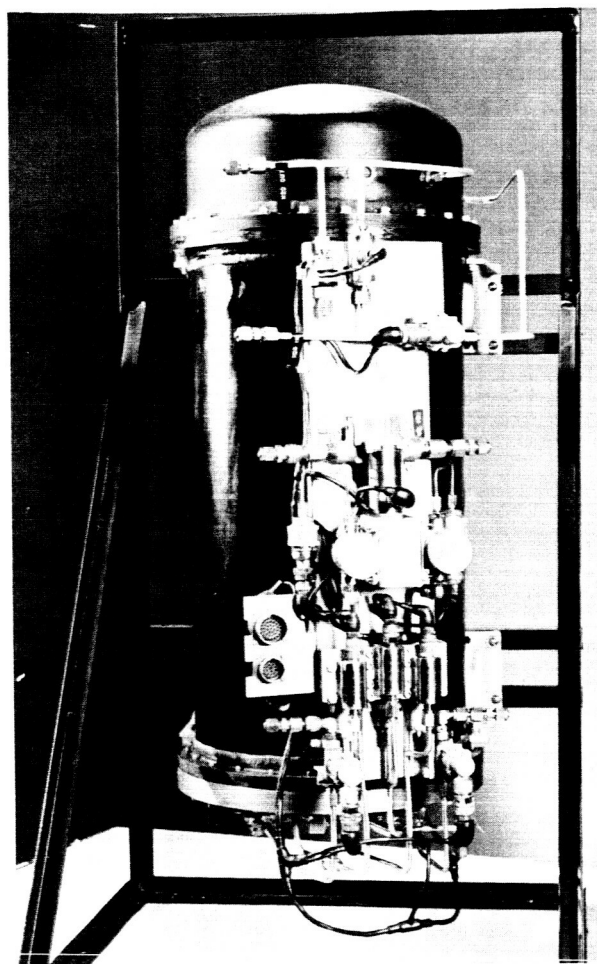


FIGURE 13. ENGINEERING MODEL SYSTEM

Figure 14 shows the special test equipment required to interface the system with the laboratory facilities.

The equipment shown is not a flight model, although the components are flight oriented. It has been heavily instrumented for test purposes; no particular attempts have been made to reduce weights or to environmentally qualify components. The control components (such as valves and transducers) shown in the foreground of Figure 13 have been mounted as removable modules on the front panel affixed to the canister housing. The entire reactant control assembly is also readily detached from the canister when particular installations require it. This feature provides accessibility to the assembly for maintenance or field repairs, which are both possible with this design.

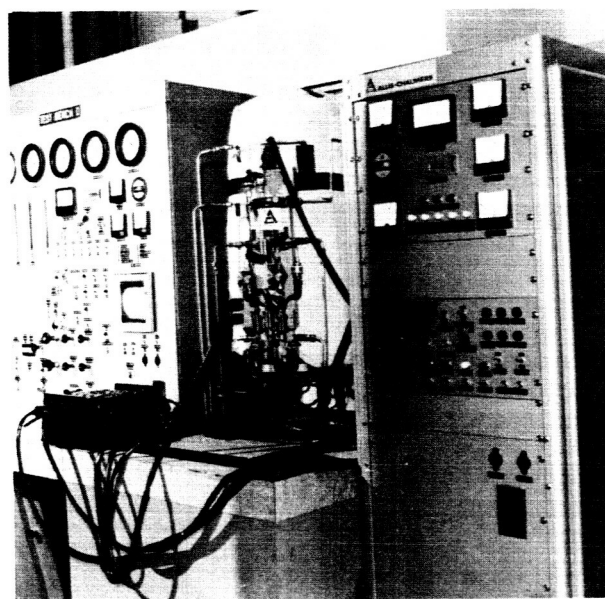


FIGURE 14. SPECIAL TEST EQUIPMENT

The rating of the delivered system is 2 kW at 29 volts, and it has an expected life well beyond the 720 hours initially designated as a design goal for this model. To achieve the 2 kW rating with the ± 2 volt regulation constraint for an output power range of 800 to 2000 watts, cells capable of sustaining current densities to 200 mA/cm^2 and having good regulation and long term stability had to be developed. This was accomplished with the incorporation of a high performance silver cathode designated as "Hysac Electrode." A typical volt-ampere characteristic for a cell with this electrode, as it would perform in a system, is shown in Figure 15; the trapezoid reflects the performance limits that an individual cell must maintain to fulfill the system requirements.

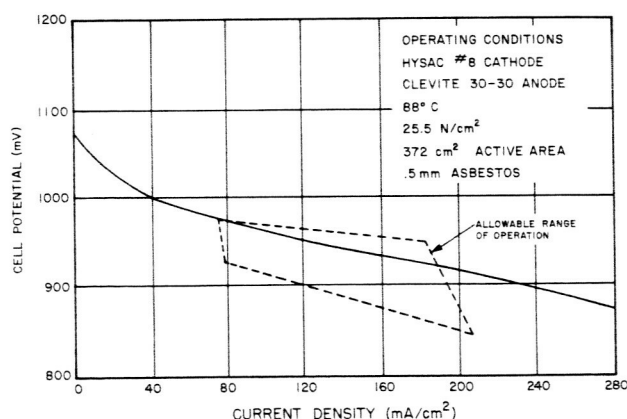


FIGURE 15. TYPICAL CELL VOLT-AMPERE CHARACTERISTIC

VII. SYSTEMS PERFORMANCE

Three extensively tested breadboard systems have shown good performance and progressive improvement and have pointed out problem areas. Breadboard systems were essentially the same as the later engineering models except that they used commercial auxiliary components and the fluid coolant subsystem was simulated with laboratory equipment. Also, the breadboards were rated for only 1800 watts. Only a brief account of these tests and the results are given here. These tests have been well documented in the quarterly reports distributed under contract NAS8-2696 (copies are available upon request).

The second breadboard system was tested at Manned Spacecraft Center using a composite load profile representing several NASA mission requirements. This profile appears in Figure 16, which shows several peaks to 1.8 kW. The system was subjected to several cycles of this profile during the first test phase, which demonstrated good performance with life to 500 hours.

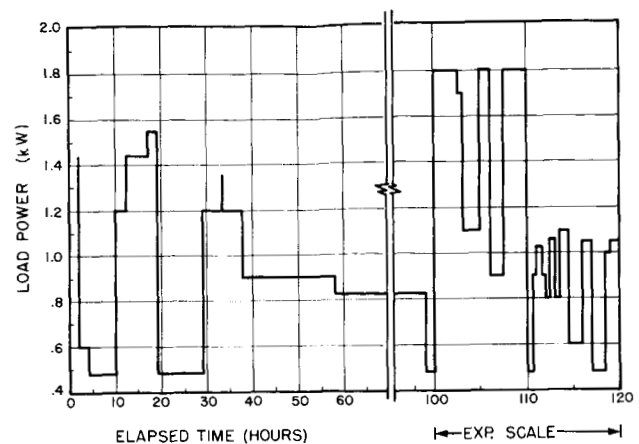


FIGURE 16. RESULTS OF BREADBOARD SYSTEM TEST

TABLE I. MISSION REQUIREMENTS VS BREADBOARD TEST RESULTS

Mission ⁽¹⁾	Mission Requirements			"35 Cell" Allis -Chalmers Breadboard Results		
		Power	Time (Hours)	Start	Hours 330	Hours 530
Gemini	total	610 to 1750 W ⁽²⁾ 23 to 30 V	340	2200 W @ 27 V	1800 W @ 26 V	1600 W @ 25 V
Apollo CSM	per mod	560 to 1420 W ⁽³⁾ 27 to 31 V	340	2200 W @ 27 V	1620 W @ 27 V	1400 W @ 27 V
LEM	per mod	130 to 1125 W 27 to 31 V	112	2200 W @ 27 V	1620 W @ 27 V	1400 W @ 27 V
Saturn	per mod	1750 W 26 to 31 V	6.5	2200 W @ 27 V	1800 W @ 26 V	

(1) Load profile for breadboard tests was a composite of requirements for all the missions listed.

(2) This peak will occur only during the two-day rendezvous missions.

(3) Emergency return one-module peak 2300 W @ 20 V (minimum).

Average power output: 3 modules 900 watts; 2 modules 1200 watts

Table I compares the output performance during the first test phase with the various mission requirements and demonstrates that the system was able to perform each of these missions. Total Gemini loads were used; whereas the Apollo, LEM, and Saturn requirements were prorated on a per module basis for these tests.

Following a long dormant period incurred by conversion of test facilities, various performance and life testing was resumed at the Manned Spacecraft Center. A useful life beyond 1000 hours was demonstrated, although the ± 2 -volt regulation desired was not maintained. This unit did not have the "Hysac Electrode" or fully automatic electrical controls. The

output characteristics of the system for several times throughout the test life are given in Figure 17.

Similar performance and life characteristics of a subsequent model tested at Allis-Chalmers are shown in Figure 17 for comparison. The notable improvement in performance shown by the latter system reflects the incorporation of "Hysac Electrodes" and automatic electrical controls and the reduction of the thickness of the electrolyte matrices from 0.0762 to 0.0508 cm. (30 to 20 mils).

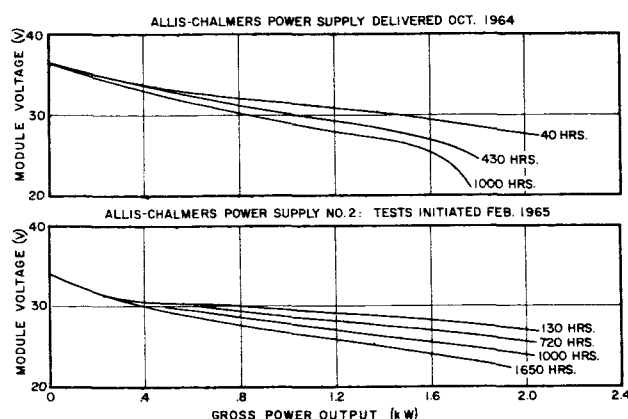


FIGURE 17. FUEL CELL OUTPUT CHARACTERISTICS

During the first 1500 hours, loads were varied between 500 and 2200 watts and held for long periods to give a total of 1,618 kWh delivered at an average load of 1.1 kW during these tests. The system maintained the ability to operate at the 2 kW level for long periods.

The thermal efficiency computed at the 400 hour mark was 65 percent for the latter system. Its specific fuel consumption to this point was 0.349 kg (0.77 lbm) per kWh. These tests demonstrated that this system, of the three compared, offers the highest energy density, the widest power range, and superior voltage regulation for longer operating times. It also was not critical to start up or shut down cycles.

VIII. FUTURE PLANS

As evidenced by the latest workscope and efforts planned for the near future by Manned Spacecraft Center, this system is considered one of the outstanding contenders, capable of improvement to meet the higher performance, reliability, and life requirements anticipated for the Apollo Applications Program.

Page intentionally left blank

THE DEVELOPMENT OF AN IMPROVED ZINC/SILVER-OXIDE BATTERY

By

Charles Graff

SUMMARY

Details of the investigations that led to the development of an improved primary zinc/silver-oxide battery are presented. Research was conducted in two areas, separator materials and variable factors. Results of the research are the development of a more effective separator system and an improved cell design.

the development of an improved primary zinc/silver-oxide battery. The primary objectives were:

1. Longer wet stand life
2. High energy-to-weight ratio
3. Low gassing
4. Good voltage regulation
5. Improved thermal characteristics.

I. INTRODUCTION

Requirements for flight batteries in the past have been for relatively high discharge rates for short periods. For these applications primary batteries with a specified wet stand of 72 hours have been used. These batteries have provided high power density and good voltage regulation.

For more recent flights, operating times have increased from minutes to hours and the vehicles have become more complex, requiring battery installation earlier in the countdown. In addition, operating procedures at Cape Kennedy require flight batteries for certain all-system testing. Recently, four sets of batteries have been required for each flight, increasing expense. Efforts have thus been directed toward development of a battery with a longer wet stand time and a limited recharge capability. If a battery can be developed that retains the desirable characteristics of the present primary battery, battery cost can be reduced significantly.

Some of these requirements are not compatible and therefore require compromise.

With the limited funds available for this program, basic materials research could not be accomplished; therefore, an attempt was made to optimize the cell design for applications using currently obtainable components. The preliminary analysis resulted in a long list of variable factors, indicating that classical research methods would not give usable results with a reasonable amount of effort and cost. It was decided to split the project into two programs. One program would be for the investigation of separator materials and combinations of separator materials and would be pursued by classical research methods since they lend themselves to this approach. The other program would consider all other variable factors and was approached by a fractional factorial analysis, which is a statistically designed experiment.

II. DEVELOPMENT PROGRAMS

In June 1963, a contract with the Eagle-Picher Company was initiated for investigations leading to

III. SEPARATOR SYSTEM

Factors such as the battery voltage, voltage regulation, battery capacity, and wet stand time are functions of the separator characteristics.

Some of the desirable characteristics of a separator material are:

1. Low electrical resistance
2. High absorbency
3. Rapid wetting ability
4. Stability of all properties over a wide temperature range
5. Stability in concentrated potassium hydroxide
6. Resistance to oxidation
7. High oxygen permissibility (less important in the primary cells)
8. Ability to retard migration of silver and zinc ions
9. Good physical strength.

The first four of these are probably the more variable among commonly used materials and lend themselves to quantitative tests. In addition to laboratory tests of the listed characteristics, some cell cycle tests were devised for the most promising separators. These preliminary tests indicated that cellulosic membranes offered advantages in electrical resistance and absorbency while polyethylene was essentially inert to the caustic environment.

Although these tests provided useful information, the ultimate tests were in the construction and operation of test cells. Also, a number of variables in cell design require optimization of the separator system or combinations of separator materials. For this evaluation, combinations of separator materials were analyzed in test cells. Post-mortem examination of these cells showed an advantage of employing an "open" material next to the positive plate. This prevents damage to the membrane by crystalline formations. These formations otherwise tend to force the separator from the plate causing uneven discharge and tearing or puncturing of the membrane.

IV. INITIAL TESTS AND DESIGN GOALS

The fractional factorial analysis of the factors not investigated in the separator program was based on Addleman's Orthogonal Main-Effect Plan No. 11 from DDC Document Number AD272250.

There are eight factors, A through H; one with four levels, one with two levels, and six with three levels. Following instructions of the Addleman plan, a matrix was set up for analysis. This resulted in a requirement for 27 trials or cells. Details of this technique are well defined in Addleman's Orthogonal Main-Effect Plan. As a result of this study, 5 duplicate sets of 18 different cell designs were discharged at different stand times. The results of these tests indicated improved capacity retention for a higher concentration of potassium hydroxide and lower density electrode material with the use of a spongy formulation of the negative material. In addition, the use of silver grids and the low density electrode materials improved the voltage of the cell.

At the completion of the study phase, it was decided to state some specific design goals. The desire was to retain the electrical characteristics of the primary cell. Specific design goals are:

1. Stand time of 30 days
2. Stand temperature of 32°C
3. Cycle capability of 6 in 30 days
 - (a) Five cycles at 25 percent depth
 - (b) Final discharge of 100 percent capacity
4. Battery voltage during discharge of 1.4 ± 0.1 volts per cell.

Data obtained during the first phase of the investigation indicated impressive stand characteristics for multiple wraps of membranes in conjunction with absorbent materials next to the positive and negative plates. Proper location of efficient, thin, separator materials permitted low cell impedance and the use of more active materials, thereby increasing capacity.

V. EXPERIMENT DESIGN

The first step in design of the experiment is to choose the significant variables as factors. Next, the number of levels of each of the quantitative and qualitative factors is chosen.

The chosen factors and their levels are:

A. Additives to electrolyte

- A₀ None
 A₁ 1% Gel
 A₂ MnO (at saturation)
 A₃ LiOH (at saturation)

B. Electrolyte Concentration

- B₀ 35%
 B₁ 40%
 B₂ 45%

C. Positive material density

- C₀ 4.155 g/cc
 C₁ 4.520 g/cc
 C₂ 4.885 g/cc

D. Positive grid metal

- D₀ 4/0 Ni
 D₁ 4/0 Ag

E. Negative material density

- E₀ 2.440 g/cc
 E₁ 2.742 g/cc
 E₂ 3.050 g/cc

F. Additive content in negative plate

- F₀ 1%
 F₁ 2%
 F₂ 4%

G. Negative grid metal

- G₀ Copper (4/0)
 G₁ Silver flashed Cu (4/0)
 G₂ Silver (4/0)

H. Negative formulation

- H₀ Pasted
 H₁ Sponge
 H₂ Metallic

The porosity, or apparent density, was very important in the formulation of both the positive and negative plates. The limiting factors in securing low density electrodes are in the formulation techniques for producing electrodes.

VI. SUMMARY OF RESULTS

In several areas, compromise was required to obtain the optimum design. The changes in the overall design of the cell are summarized in the list below, which gives a comparison of the construction before and after development.

	PRESENT	IMPROVED
Positive Grid	Nickel	Silver
Silver Density	4.885-5.490 g/cc	4.270-4.575 g/cc
Negative Grid	Copper	Silver
Positive Absorbent	None	6.35 x 10 ⁻³ cm matted nylon
Membrane	#133 Visking	Two Thin Cellulose
Negative Absorbent	20.32 x 10 ⁻³ rayon	6.35 x 10 ⁻³ cm rayon

The most promising achievements are a more effective separator system, moderate recharge capabilities, and a smaller overall thickness. This allows the use of more active materials and actually increases the capacity of the cell. In addition, improved design and formulation of the plates increased the capacity.

A comparison of the discharge characteristics of the two cells is shown in Figure 1.

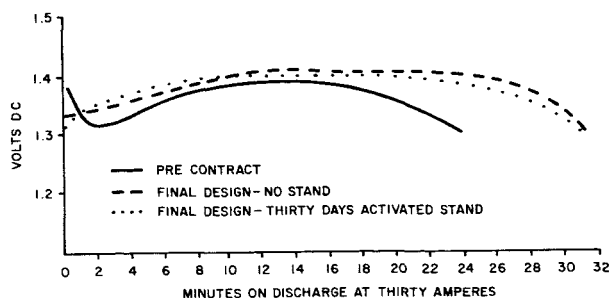


FIGURE 1. TYPICAL DISCHARGE CHARACTERISTICS, THIRTY AMPERES AT +23.9° C

Note that initial voltage in the cell after 30 days stand is a little higher than the cell with no stand time. This is probably the result of a higher charge state after the last partial discharge.

Future plans are to put some of the improved cells into a multi-cell battery to check the validity of the single cell test and also to build cells with larger electrode areas to see what type of scale-up problem might develop.

N66 32609

THE ELECTRICAL POWER SYSTEM FOR THE PEGASUS SATELLITE

By

Charles Graff

SUMMARY

The electrical power system developed for the Pegasus satellite by Fairchild Hiller with assistance provided by the Astrionics Laboratory of MSFC is described.

The power load for Pegasus is approximately 40 watts, with peaks occurring during interrogation intervals. Electrical power is provided by a photovoltaic, secondary battery power system. Solar energy conversion is accomplished with silicon solar cells. A battery with a nominal capacity of 6 ampere-hours provides power during the dark period, which varies between 35 and 15 minutes. Dual battery and recharge systems are provided.

Three Pegasus satellites are now in orbit with the power systems functioning properly.

I. INTRODUCTION

The Pegasus satellite was developed under contract by Fairchild Hiller. Astrionics Laboratory closely monitored and provided assistance in the development of the electrical power system.

The Pegasus satellite is an excellent example of the application of a photovoltaic, secondary battery power system. The load is approximately 40 watts with peaks occurring during interrogation intervals. The orbit is approximately 100 minutes with eclipse ratio variations from 35:65 to 15:85.

II. EQUIPMENT DESCRIPTION

A 23-cell nickel-cadmium battery with a nominal capacity of 6 ampere-hours was selected to provide power during the dark period. During the maximum eclipse time of 35 minutes, the load is supplied with 13 percent of the battery capacity.

The solar energy conversion for this satellite is accomplished with N-on-P silicon solar cells on four panels. The panels are deployed in orbit in the planes of a regular tetrahedron, giving maximum area utilization efficiency for solar cell panels on a randomly oriented satellite. The average power available during random orientation is 79 percent of the maximum from one panel.

The forward solar panel is 103.14 by 163.83 centimeters and contains 6160 solar cells in an arrangement of 55 parallel strings of 112 in series. Under test conditions at Table Mountain, California, the panel produced 115 watts at 42 volts. In orbit, the maximum power per panel is approximately 135 watts, and the average power from all four panels is approximately 110 watts. During the sunlit portion of the orbit, the solar cells power the 40-watt load directly while simultaneously charging the batteries. Approximately 48 watts are required for battery charging and about 20 watts are dissipated in the power-system electronics.

Figure 1 shows a block diagram of the entire Pegasus electrical power system. The four solar cell panels are connected through diodes to prevent back-loading through unilluminated panels.

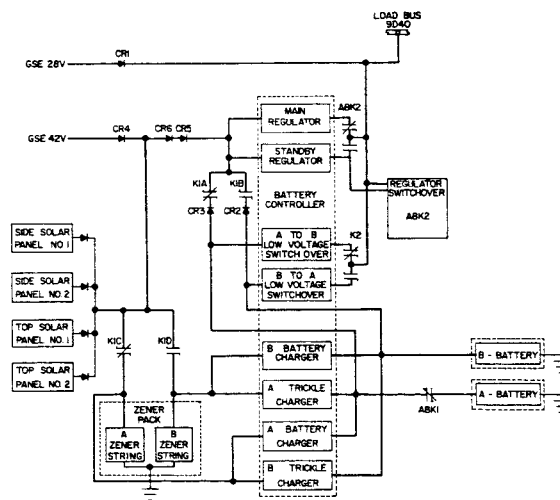


FIGURE 1. BLOCK DIAGRAM OF PEGASUS POWER SYSTEM

Ground support equipment inputs simulate both solar cell power at 42 volts and the battery power at 28 volts. The rest of the power system is fully redundant with dual batteries, chargers, and regulators and with automatic switchover capability if any unit malfunctions. The regulator switchover circuit monitors the load bus voltage and switches to the standby regulator if the voltage exceeds 35 volts or drops below 24 volts. The battery switchover circuits are activated through ground command. Once activated, the switchover is effected if the voltage drops below 24 volts. A ground-transmitted activation command prevents continuous switching back and forth if both batteries degrade to low voltage. Each battery has a main battery charger and a trickle charger; these are switched in pairs as the batteries are switched. Also, each pair of chargers has its own 42-volt zener diode voltage-limiting circuit which is also switched.

III. BATTERY RECHARGE

The battery recharge philosophy was derived from two major considerations. The first was to insure adequate recharge during the minimum orbital sunlight time of 65 minutes, and the second was to protect the battery from excessive gas buildup during the overcharge period.

To safely recharge the battery in the minimum 65-minute recharge time, it is necessary to charge at as high a current as allowable. Figure 2 shows the maximum allowable overcharge currents and voltages as functions of temperature which prevent the Pegasus battery from gassing excessively. It also shows that at high temperature the charge current may be large but the battery can be charged only to a relatively low terminal voltage.

In Figure 3, the family of battery charger characteristic curves show that the voltage reaches its maximum safe limit before the charge current is reduced. The charger uses three types of feedback (current, voltage, and battery temperature) to accomplish this. Through this approach we obtain the maximum advantage of the battery's capability of using a higher recharge current at low temperatures. This technique provides maximum reliability and optimum economy of solar cell power.

The trickle chargers are constant-current

devices with either a 100 mA or 500 mA capability. The normal mode is to maintain the standby battery on a 100 mA trickle charge. If the battery temperature should go high and increase the internal self-discharge current so that 100 mA will not maintain peak charge, the 500 mA rate may be switched in through ground command. The 500 mA rate will also be switched in after a battery switchover to revive the degraded battery.

The three Pegasus satellites are now in orbit and, to the best of our knowledge, the power systems are functioning properly.

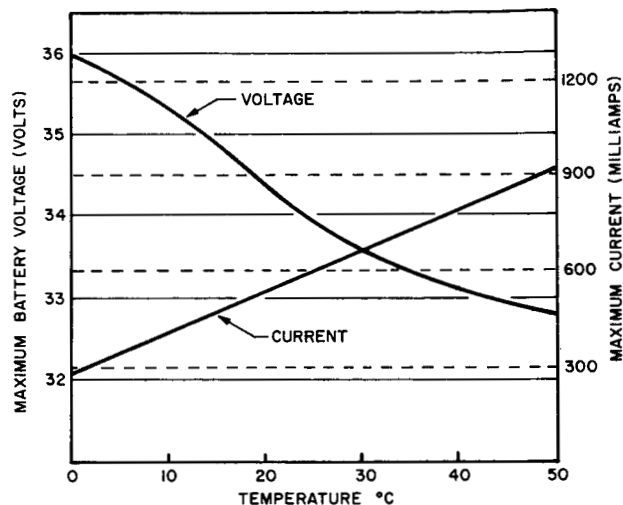


FIGURE 2. MAXIMUM OVERCHARGE AND CURRENT ALLOWABLE FOR PEGASUS BATTERY

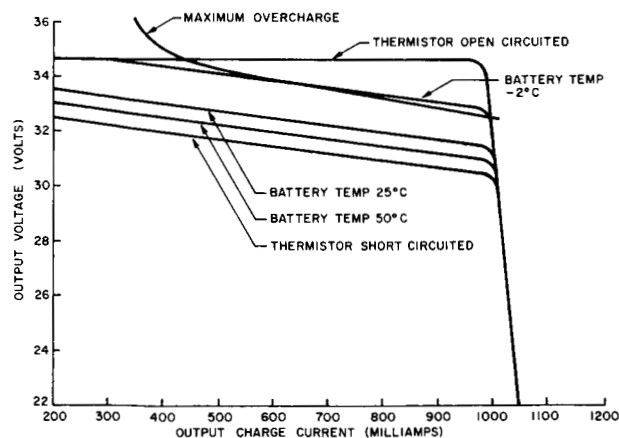


FIGURE 3. BATTERY CHARGER CHARACTERISTICS AND OVERCHARGE LIMITS

N66 32610

BRUSHLESS DC MOTORS

By

Dwight Baker

SUMMARY

Two brushless dc motor systems being used extensively in many space programs are described; the basic principles of operation of each are compared. In addition, the brushless dc motor and the conventional dc motor are compared, and the major advantages of each are discussed.

The present and proposed uses of brushless dc motors by MSFC are included to indicate the major advantages and future applications of these systems. Several future research and development tasks are proposed to indicate the additional efforts needed to meet the requirements for future programs.

I. INTRODUCTION

Many of the space programs require specialized motor-drive systems for liquid pumps, blowers, lunar vehicle drive systems, etc. To meet these requirements, development of improved drive systems capable of operating in the severe environments imposed by space missions will be necessary. Effort must be directed toward improved performance, high reliability, efficient operation over wide speed and load ranges, and improved maintenance-free operation for extended periods.

Because the primary electrical power sources of space vehicles are generally low voltage, dc types, motor system operation must be compatible with these limited capacity dc sources.

To provide for the existing and future requirements of these motor systems, MSFC has investigated and performed preliminary research and development on several of the brushless dc motor concepts. These

efforts clearly indicate that brushless motors offer major advantages over conventional dc motors for many applications.

Most of the present brushless dc motor designs for space vehicles are limited to output power levels of a few hundred watts. This limitation is primarily caused by the lack of proper motor designs and of power transistors capable of switching the required current levels. Recent improvements in power semiconductor devices, electronic control techniques, and motor designs now make it possible to develop reliable motor systems rated at several kilowatts.

The term "brushless dc motor" does not necessarily indicate that the motor has the operating characteristics of conventional dc motors but only that the input to the system is a dc voltage and that the motor does not incorporate brushes for commutation.

II. COMPARISON OF BRUSHLESS DC MOTORS

Brushless dc motors may be divided into two major classifications, each subdivided according to the method used to control the motor. The motor types and control schemes which are now being used extensively are listed in Table I.

TABLE I. MOTOR TYPES AND CONTROL SCHEMES

- | |
|--|
| A. Dc/ac-inverter-driven induction motor |
| 1. Fixed frequency inverter |
| 2. Variable frequency inverter |
| B. Rotor-position-sensing motor |
| 1. Photoelectric sensor |
| 2. Reluctance switch sensor |
| 3. Hall generator sensor |

The first type listed is an ac induction machine driven by an inverter that changes the dc input voltage to an ac square wave source by means of electronically controlled switching elements.

The second type employs basic dc machine principles of operation and incorporates electronic commutators in lieu of brushes and commutating bars.

The inverter induction-motor combination requires the inverter to convert the dc input voltage into an alternating source suitable for driving the motor. The inverter output voltage and frequency are controlled by the inverter; since semiconductor devices are normally used as output switches, the output waveform is a square or quasi-square wave. A significant improvement in system efficiency is realized by using this type of drive for the motor.

An elementary block diagram of a typical fixed frequency inverter induction-motor system is shown in Figure 1. The input voltage is connected to the

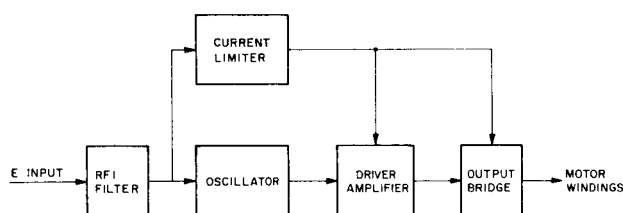


FIGURE 1. BLOCK DIAGRAM OF INVERTER INDUCTION MOTOR

oscillator, which controls the inverter operating frequency. The output signal from the oscillator is amplified by the driver amplifier and used to drive the output bridge stage. The induction motor windings are connected directly to the output bridge. The current limiter is required to limit the input current to an acceptable level during motor starting and stalled conditions.

Many variations in the design of the inverter induction-motor system are possible and depend on the application and method of implementation. By proper control of the motor voltage and frequency, efficient speed and torque control can be achieved over extremely wide operating ranges. In addition, the number of phases can be selected to provide optimum performance. Although more complex, multiple phase systems normally provide the advantages of higher starting torque, increased efficiency, lower harmonic content, and less electrical noise generated.

All motors of the rotor-position-sensing type are essentially the same although the method used to sense the rotor position may differ considerably. The maximum torque in the basic dc motor is produced when the armature and rotor fields are displaced by 90 electrical degrees. In this motor the position of the rotor is sensed and the sensing device produces an electrical signal that is used to maintain an approximate 90-degree relationship by activating the proper electronic commutating devices. Although a reluctance motor could be used for low power application, permanent magnets are generally used for the rotor because of the increased efficiency; therefore, the armature is the stator, i.e., opposite to that of a conventional dc motor.

A functional block diagram of a typical rotor-position-sensing motor appears in Figure 2. The

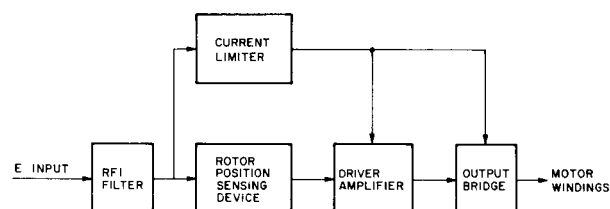


FIGURE 2. BLOCK DIAGRAM OF ROTOR POSITION SENSING MOTOR

only difference between this diagram and that of Figure 1 is that the oscillator section is replaced by the rotor-position-sensing device. Therefore, the output bridge frequency is controlled by the rotor speed in Figure 2, whereas the bridge frequency of Figure 1 is controlled completely by the oscillator stage.

The elementary circuit diagram shown in Figure 3 depicts a typical output bridge stage coupled to a three-phase motor. Note that the motor windings are connected directly to the bridge and require no transformer for coupling. This, however, normally requires a special motor winding because of the relatively low source voltage available. By eliminating the coupling transformer, an improvement in the size, weight, and efficiency of the system is normally realized.

The circuit of Figure 3 may be used for driving either the induction motor or the rotor-position-sensing motor. In the former case, the frequency is determined by the inverter design; for the latter case, the frequency is determined by the rotor through a feedback system that controls the commutators.

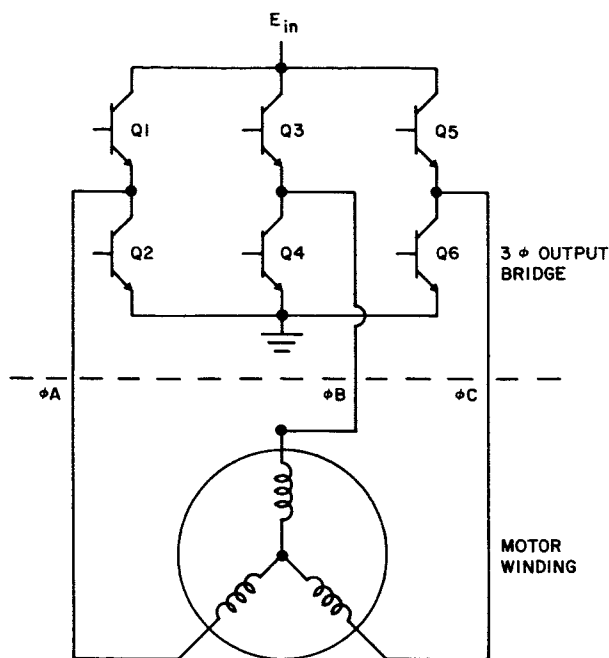


FIGURE 3. TYPICAL 3 ϕ OUTPUT BRIDGE AND MOTOR WINDING

A typical output bridge sequence and the resultant motor waveform for the circuit of Figure 3 are illustrated in Figure 4. This quasi-square wave has proven to be very satisfactory for driving properly designed motors.

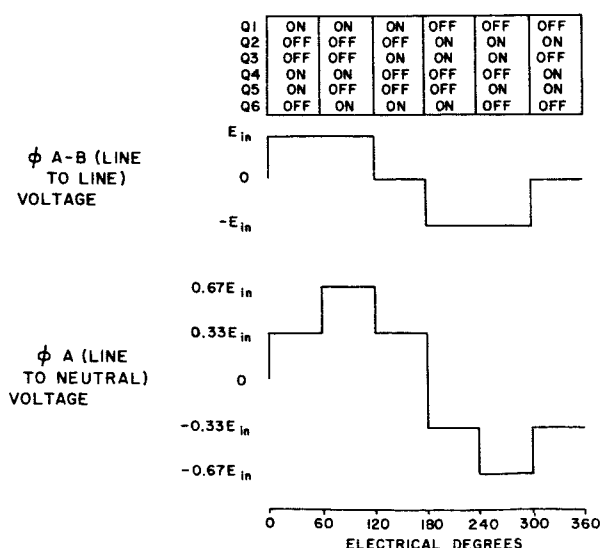


FIGURE 4. TYPICAL TRANSISTOR SEQUENCING AND MOTOR WINDING WAVEFORMS

III. COMPARISON OF BRUSHLESS AND CONVENTIONAL DC MOTORS

Although the brushless dc motor has only recently been used extensively in space vehicles, many significant improvements in performance over conventional dc motors have already been realized for many applications.

A. ADVANTAGES OF THE BRUSHLESS DC MOTOR

1. Operation in environments, such as vacuum, explosive, and high vibration, that forbid the use of conventional brushes.
2. Increased operating time without maintenance. No replacement of the electronic switching components should be necessary during the motor lifetime.
3. Efficient speed and torque control. Recently developed control techniques provide more efficient speed and torque control than obtained in the conventional dc motor for many applications.
4. Low control power. The brushless design requires extremely low control power for controlling the motor speed, torque, direction of rotation, etc.
5. Inverter or commutating devices may be located remote from the motor. In the event the motor environment is too severe, the electronic section may be located remote from the motor housing in a controlled environment.

6. Redundancy. Since the commutators are semiconductor devices, manual or automatic redundancy of the electronic section may be incorporated.

7. Reduced radio frequency interference. Arcing does not occur during electronic commutation.

B. DISADVANTAGES OF THE BRUSHLESS DC MOTOR

The major disadvantages of the brushless dc motors for most applications are:

1. Lower efficiency
2. Increased size and weight
3. Increased complexity.

Although these disadvantages normally apply to the motor design, use of the brushless motor design will often result in an improvement of system size, weight, efficiency, and complexity. As an example,

for conventional dc motor operation in a vacuum environment, it is often necessary to create an artificial environment suitable for brush operation. This usually results in a significant increase in system size, weight, and complexity.

IV. BRUSHLESS DC MOTORS FOR SATURN IB AND V VEHICLES

The following lists the present uses of brushless dc motors for the Saturn IB and V vehicles.

1. Environmental control system (ECS) coolant pump for the Instrument Unit. The ECS coolant pump motor is a rotor-position-sensing type which uses the photoelectric method of commutation control. This is a 3-phase, 400-watt motor operating from a 28-volt dc input power source.

2. LH_2 and LO_2 chilldown pumps for the S-IVB stage. This system uses the inverter/induction-motor system operating from a 56-volt dc source. This is a 3-phase motor rated at approximately 750 watts. The induction motor operates submerged in the LH_2 and LO_2 .

3. LH_2 chilldown pumps for the S-II stage. This motor is essentially the same as item 2.

V. PROPOSED BRUSHLESS DC MOTOR APPLICATIONS

The following lists the proposed applications for the brushless dc motor.

1. Blowers for fuel cell cooling systems. This system will use the inverter/induction-motor combination. The motor will be a 2-phase unit rated at approximately 50 watts of output power and will operate from a 28-volt dc source.

2. Auxiliary hydraulic pump for the Saturn IB and V vehicles, S-IVB stage. The exact motor system has not been defined, but the motor will operate from a 56-volt dc source and will be required to deliver approximately 3.3 kilowatts.

3. Wheel drive for lunar vehicles. Although the exact motor requirements have not yet been determined, preliminary investigation indicates that the brushless dc motor (inverter/induction-motor combination with special controls) offers many desirable features for this application.

VI. FUTURE RESEARCH AND DEVELOPMENT REQUIREMENTS

Even though the brushless dc motor is already being used extensively in present space programs, many improvements for the system size, weight, efficiency, and reliability are urgently needed. The following are some of the development tasks that are essential to provide brushless designs capable of meeting the future missions.

1. High powered systems. Future programs will undoubtedly require higher powered systems than those presently available.

2. Redundant techniques. Future missions, such as lunar exploration, will place emphasis on reliability for extended operating times. This will certainly require the use of automatic and manual redundancy techniques.

3. Efficient current limiting techniques. Efficient methods of limiting the input current to safe levels during starting and stalled operation must be developed. Most present designs incorporate inefficient, brute-force current limiting schemes.

4. Variable frequency inverter/induction-motor systems. To provide excellent speed and torque control, variable frequency inverters and associated control circuitry must be developed.

5. System for wheel drive application. Future programs will require the development of electrical wheel drive systems capable of operating over wide speed and load ranges. In addition, efficient control techniques for controlling the speed, torque, direction of rotation, etc., of these wheels must be developed.

SINGLE-ENDED SWITCHING TRANSFORMER REGULATOR

By

Dwight Baker

SUMMARY

This paper describes the theory of operation of a single-ended switching transformer regulator capable of providing a highly regulated, electrically isolated output voltage. It also discusses the principal advantages of this technique over conventional methods. Electrical design calculations and procedures are included to assist the circuit designer in designing efficient, compact, and reliable dc-to-dc converters for specific applications.

A general circuit description and those equations considered pertinent in providing the necessary design information are included. Detailed mathematical analysis is not deemed necessary; therefore the design equations consider the components as idealized and neglect insignificant terms such as the resistance of the transformer winding, voltage drop across a saturated transistor, input source impedance, etc. Because component tolerances normally introduce the greater error in the final design, this consideration is valid.

LIST OF SYMBOLS

V_0	output voltage (volts)	V_{CE}	transistor collector-to-emitter voltage during time $T_2 - T_1$ (volts)
V_1	primary winding N_1 voltage during time $T_2 - T_1$ (volts)	V_{CR1}	forward voltage drop across diode CR1 (volts)
V_2	secondary winding N_2 voltage during time $T_2 - T_1$ (volts)	V_R	diode reverse voltage (volts)
V'_2	voltage induced in winding N_2 during time T_1 (volts)	V'_R	voltage ripple across capacitor C1 caused by capacitor impedance (volts peak to peak)
V_3	voltage induced in the sense winding (volts)	V''_R	voltage ripple across capacitor C1 caused by energy transfer (volts peak to peak)
		i	current through N turns (amperes)
		I_1	peak transistor collector current (amperes)
		I_2	peak current in winding N_2 (amperes)
		L_1	inductance of transformer winding N_1 (henries)
		L_2	inductance of transformer winding N_2 (henries)
		N	number of transformer turns
		N_1	number of transformer primary turns
		N_2	number of transformer secondary turns
		N_3	number of turns in sense winding
		W_1	energy stored in transformer at and of time T_1 (joules)
		W_2	energy delivered by the transformer during time $T_2 - T_1$ (joules)

T_1	time required to store energy in transformer
$T_2 - T_1$	time required to deliver the stored energy (seconds)
T_3	period of one cycle (seconds)
P_I	input power (watts)
P_0	output power (watts)
Z_L	load impedance (ohms)
Z_c	capacitor impedance (ohms)
R_L	load resistance (ohms)
η	converter efficiency
ϕ	flux (webers)
k	constant of proportionality

I. INTRODUCTION

Some of the major problems of the conventional push-pull converter are discussed to show the merits of the single-ended switching transformer regulator.

Figure 1 is the basic circuit of the conventional push-pull converter; typical transistor voltage and current waveforms are included for reference during the following discussion.

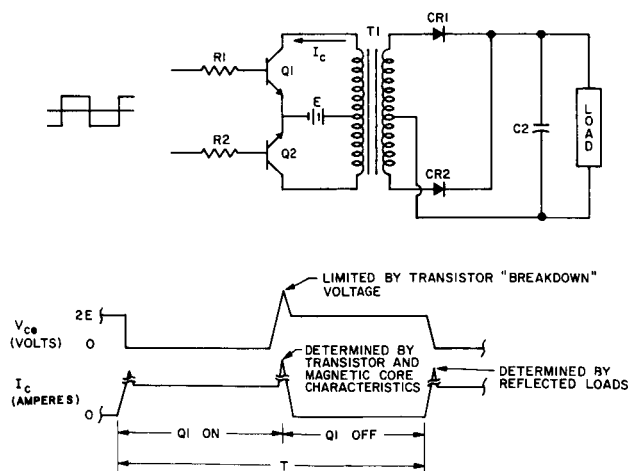


FIGURE 1. CONVENTIONAL METHOD OF DC-TO-DC CONVERSION

Unpredictable current and voltage transients occurring during the transistor switching time each half cycle contribute to inefficient operation and often lead to catastrophic failure.

The major causes of the conditions are:

1. Transistor "crossover" currents. Because of the switching characteristics of the transistor, both transistors conduct current simultaneously during the switching time and produce a current peak in these components each half cycle. The magnitude and duration are dependent on several factors such as the transistor storage time, rise and fall times, current gain, temperature, and loading effects. These factors vary with each component and it is extremely difficult, if not impossible, to eliminate this transient condition without affecting the performance or increasing the complexity of the design significantly.

2. Saturation of the magnetic core material. Symmetrical operation of the transformer requires that the product of the voltage applied to the transformer winding and the time this voltage is applied be identical each half cycle. Exact symmetry obviously cannot be achieved because of differences in the saturation voltages and switching characteristics of the transistors. Provided sufficient imbalance exists, the "square hysteresis loop" core material normally used in this type of design will saturate during each cycle of operation and produce a surge current in one of the transistors. Again, the amplitude and duration of the current transient will depend on factors such as the transistor, magnetic core, power source, and transistor drive characteristics.

3. Load reflection to primary winding. In the conventional transformer operation, the secondary loads will be continuously reflected to the primary and, in certain applications, will produce transient loading effects in the transistors. In addition, the diode capacitance in the rectifier bridge will reflect an extremely low impedance to the primary winding during the switching time each half cycle and cause current transients in the transistors.

4. Voltage transients. The leakage inductance of the transformer windings will normally produce a voltage transient across the transistor of sufficient magnitude to force the component into a secondary breakdown condition each cycle. This condition does not normally lead to a catastrophic failure, provided the transistor sustaining voltage is sufficiently high; it does result in additional power dissipation in the device.

5. Radio frequency interference (RFI) considerations. The design of the adequate RFI filters capable of suppressing the radiated and conducted interference levels is further complicated when several dc-to-dc converters of the same design are required, because the transient current conditions will vary with each component.

The foregoing discussion has described briefly several undesirable features of the push-pull principle of operation and leads to the conclusion that both current and voltage transients often affect the performance and reliability of the design.

II. THEORY OF OPERATION

Figure 2 is the basic single-ended switching transformer dc-to-dc converter developed by MSFC for transferring electrical energy from the input power source E_1 to the electrically isolated output load. In

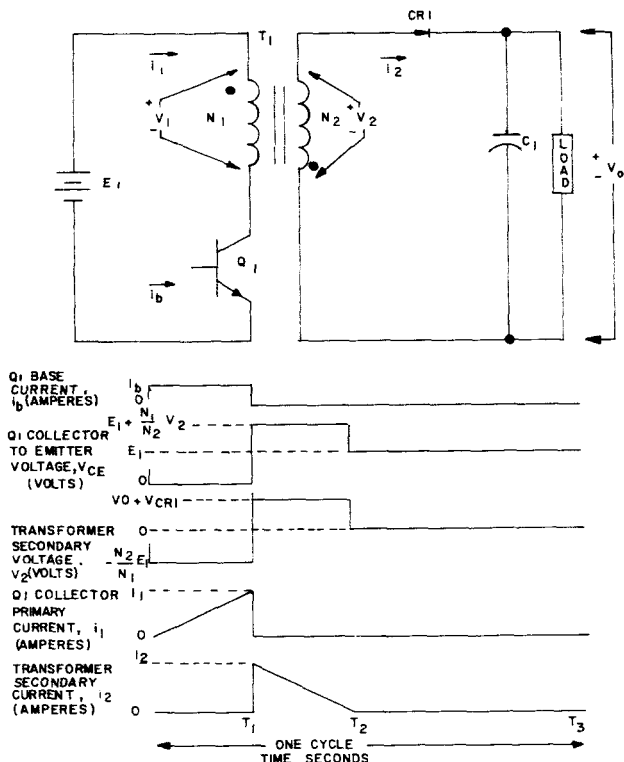


FIGURE 2. SINGLE-ENDED SWITCHING TRANSFORMER DC-TO-DC CONVERTER

addition to merely converting the input power to the desired output level, extremely accurate voltage regulation can be maintained by proper control of the switching frequency of transistor Q_1 . It should be emphasized that electrical power conversion, electrical output isolation, and voltage regulation can be accomplished in only one "stage" of operation requiring few components. Conventional methods normally require more than one stage and a significant increase in components to accomplish comparable results.

The transistor Q_1 is driven into the saturated state for a specific period of time T_1 ; this connects the input power source directly across the transformer primary winding N_1 . The voltage V'_2 induced into the secondary winding N_2 during time T_1 is expressed as

$$V'_2 = \frac{N_2}{N_1} E_1. \quad (1)$$

The secondary winding, phased as shown in Figure 2, results in diode CR_1 blocking current flow in the transformer secondary winding during time T_1 . Since no power is delivered by the transformer secondary winding during this time, the transformer may be regarded merely as an inductor consisting of N_1 turns and the magnetic core. All components except the inductor, transistor, and input power source may be disregarded, as shown in Figure 3.

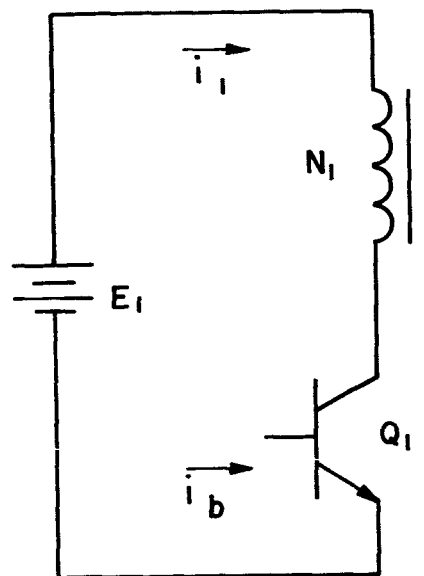


FIGURE 3. SIMPLIFIED CIRCUIT FOR TIME T_1 OPERATION

The equation for the primary current through the transistor may be calculated from the basic equation:

$$E_1 = L_1 \frac{di_1}{dt} \quad (2)$$

or

$$I_1 = E_1 \int_0^{T_1} \frac{1}{L_1} dt. \quad (3)$$

For the magnetic materials that exhibit a constant inductance with varying magnetomotive forces, equation (3) may be written as

$$I_1 = \frac{E_1 T_1}{L_1} \quad (4)$$

Experimental results verify that the low permeability (60μ) Permalloy powdered magnetic cores presently being used in this design maintain a relatively constant inductance for magnetomotive forces up to about 40 A/cm (50 oersteds), which includes the normal operating range for present applications. From equation (4), the peak transistor current is proportional to the time the transistor remains in the saturated state. It is most important to note that the peak collector current in the transistor is completely independent of the output load (any value between a short and open circuit condition) and is determined solely by time T_1 for applications where E_1 is constant. By controlling this time to the desired fixed value, we can adjust the peak transistor current I_1 (Fig. 2) to correspond to the capabilities of the transistor with assurance that this value will not be exceeded during any phase of operation.

At time T_1 , Q1 is switched to the OFF state causing a reversal of the flux change in the transformer. This action produces an induced voltage in each winding (N_1 and N_2) proportional to the number of turns and of opposite polarity to the polarity during time T_1 .

The voltage induced into the winding N_2 will be clamped to the sum of the output voltage and the forward voltage drop across diode CR1.

$$V_2 = V_0 + V_{CR1} \quad (5)$$

The voltage induced into the primary winding N_1 is given by

$$V_1 = \frac{N_1}{N_2} V_2 \quad (6)$$

or

$$V_1 = \frac{N_1}{N_2} (V_0 + V_{CR1}) \quad (7)$$

The transistor collector-to-emitter voltage during time $T_2 - T_1$ is the sum of the input voltage and the primary winding voltage:

$$V_{CE} = E_1 + V_1 \quad (8)$$

or

$$V_{CE} = E_1 + \frac{N_1}{N_2} (V_0 + V_{CR1}) \quad (9)$$

Since E_1 , V_0 , and V_{CR1} are relatively constant for a particular application, the voltage applied across the transistor collector-to-emitter terminals can be controlled by proper selection of the turns ratio $\frac{N_1}{N_2}$ to a level which will ensure freedom from secondary breakdown of the transistor. Equation (9) does not account for the low energy stored in the leakage inductance, which will produce a voltage transient across Q1, but this voltage can be controlled by incorporating a zener diode across the collector-to-emitter terminals of Q1 or by other transient suppression techniques. The value of the zener voltage must be between the value calculated in equation (9) and the secondary breakdown voltage of Q1.

During time $T_2 - T_1$, Q1 is in the nonconducting state and no electrical power is transferred by the primary winding N_1 . The transformer can therefore be regarded merely as an inductor with N_2 turns. For circuit analysis during this time, all circuitry of Figure 2 may be disregarded with the exception of CR1, C1, the load, and the inductor as shown in Figure 4.

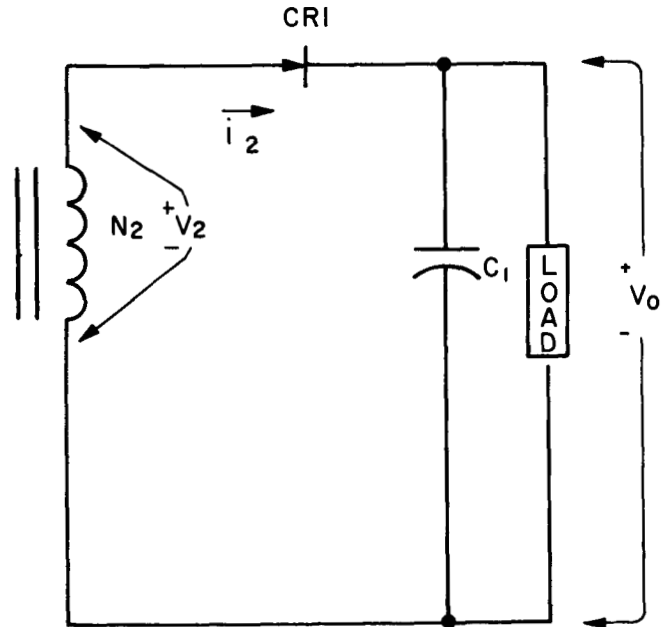


FIGURE 4. SIMPLIFIED CIRCUIT FOR TIME $T_2 - T_1$ OPERATION

At time T_1 , the electrical energy stored in the transformer core material is given by the basic equation

$$W_1 = \frac{1}{2} L_1 I_1^2 \quad (10)$$

The energy delivered by the transformer during time $T_2 - T_1$ is given by

$$W_2 = \frac{1}{2} L_2 I_2^2. \quad (11)$$

Since the energy stored during time T_1 must be equal to the energy delivered during time $T_2 - T_1$, equations (10) and (11) can be combined to calculate the peak current in winding N_2 at time T_1 :

$$\frac{1}{2} L_1 I_1^2 = \frac{1}{2} L_2 I_2^2 \quad (12)$$

$$I_2 = \sqrt{\frac{L_1}{L_2}} I_1. \quad (13)$$

The inductance of the transformer with N_2 turns may be calculated by considering that the magnetic flux is proportional to the magnetomotive forces. This is a valid assumption for the core material presently being used for this application, provided the transformer operating range is restricted as discussed previously.

Therefore,

$$\phi = kNi \quad (14)$$

or

$$i = \frac{\phi}{kN}. \quad (15)$$

Therefore,

$$\frac{di}{dt} = \frac{1}{kN} \frac{d\phi}{dt}. \quad (16)$$

By combining the basic equation

$$e = L \frac{di}{dt} \quad (17)$$

with equation (16), we obtain

$$e = \frac{L}{kN} \frac{d\phi}{dt}. \quad (18)$$

The general law for induced voltage is

$$e = N \frac{d\phi}{dt}. \quad (19)$$

Combining equations (18) and (19) yields

$$L = kN^2. \quad (20)$$

Equation (20) verifies that the inductance of the transformer is proportional to the square of the turns.

Therefore,

$$\frac{L_1}{L_2} = \frac{N_1^2}{N_2^2}. \quad (21)$$

Combining equations (13) and (21) yields

$$I_2 = \frac{N_1}{N_2} I_1. \quad (22)$$

Equation (22) shows that the peak current through winding N_2 is dependent only on the peak primary current I_1 and the transformer turns ratio N_1/N_2 .

The time ($T_2 - T_1$) required to discharge the transformer stored energy may be determined by considering the basic magnetic equation

$$V_2 = L_2 \frac{di_2}{dt}. \quad (23)$$

Since V_2 and L_2 are both essentially constant, the slope $\frac{di_2}{dt}$ may be considered constant.

Therefore, equation (23) may be written as

$$\frac{I_2}{T_2 - T_1} = \frac{V_2}{L_2}. \quad (24)$$

The time required to deliver the stored energy is given by rearranging equation (24) as follows:

$$T_2 - T_1 = \frac{I_2 L_2}{V_2}. \quad (25)$$

Therefore, the equation of the secondary winding current i_2 is

$$i_2 = I_2 - \frac{V_2}{L_2} (t - T_1) \quad (26)$$

where $T_1 \leq t \leq T_2$.

When equations (4) and (25) are combined, the ratio of the time ($T_2 - T_1$) required to discharge the transformer to the time T_1 required to store the energy is given by

$$\frac{T_2 - T_1}{T_1} = \frac{I_2 L_2}{V_2} \frac{E_1}{L_1 I_1}. \quad (27)$$

By combining equations (21), (22), and (27), we obtain

$$\frac{T_2 - T_1}{T_1} = \frac{I_1 E_1}{I_2 V_2} \quad (28)$$

or

$$\frac{T_2 - T_1}{T_1} = \frac{N_2 E_1}{N_1 V_2} \quad (29)$$

The input power to the switching regulator is given by the basic equation,

$$P_I = \frac{1}{T_3} \int_0^{T_1} e_1(t) i_1(t) dt \quad (30)$$

The input voltage $e_1(t)$ is a constant E_1 and $i_1(t) =$

$$\frac{I_1 t}{T_1}.$$

Therefore, equation (30) may be written as

$$P_I = \frac{E_1 I_1}{T_1 T_3} \int_0^{T_1} t dt \quad (31)$$

$$P_I = \frac{E_1 I_1}{2} \frac{T_1}{T_3} \quad (32)$$

From equation (32), the input power is directly proportional to the transistor duty cycle T_1/T_3 .

In the normal operating condition, sufficient time is permitted for the transformer to deliver all stored energy prior to allowing the transistor to conduct. For this condition the maximum duty cycle can be determined as follows ($T_2 = T_3$):

$$\frac{T_1}{T_3} = \frac{T_1}{T_2} = \frac{T_1}{T_1 + (T_2 - T_1)} \quad (33)$$

Combining equations (4) and (25) yields

$$\frac{T_1}{T_2} = \frac{\frac{I_1 L_1}{E_1}}{\frac{I_1 L_1}{E_1} + \frac{I_2 L_2}{V_2}} \quad (34)$$

or

$$\frac{T_1}{T_2} = \frac{1}{1 + \frac{I_2 L_2 E_1}{I_1 L_1 V_2}} \quad (35)$$

Combining equations (21), (22), and (35) yields

$$\frac{T_1}{T_2} = \frac{1}{1 + \frac{N_2 E_1}{N_1 V_2}} \quad (36)$$

Combining equations (6), (8), and (36) yields

$$\frac{T_1}{T_2} = \frac{V_{CE} - E_1}{V_{CE}} \quad (37)$$

Therefore, the maximum input power to the switching regulator is given by combining equations (32) and (37) ($T_2 = T_3$ for maximum duty cycle).

$$P_I = \frac{E_1 I_1}{2} \frac{V_{CE} - E_1}{V_{CE}} \quad (38)$$

The maximum output power can be determined as follows:

$$P_0 = \eta P_I = \eta \frac{E_1 I_1}{2} \frac{V_{CE} - E_1}{V_{CE}} \quad (39)$$

Equation (39) will provide the designer with a quick means for calculating the maximum output power, provided the efficiency η can be adequately predicted. Although the efficiency is a function of several factors including the input voltage level, operating frequency, and circuit components, a satisfactory estimate can normally be made.

III. OUTPUT FILTER

The output ripple across the filter capacitor is produced by two factors: (1) the product of the peak current through the capacitor and the capacitor impedance, and (2) the energy that is transferred to the capacitor will naturally increase the output voltage and results in an output voltage variation. The ripple produced by the product of the peak capacitor current and the capacitor impedance is given by

$$V'_R = (I_2 - \frac{V_0}{Z_L}) Z_C \quad (40)$$

The ripple resulting from the electrical energy transfer to the capacitor is given by equating the energy delivered to the capacitor to the energy delivered by the transformer minus the energy used in the load:

$$\frac{1}{2} C_1 (V''_R)^2 = \frac{1}{2} L_2 I_2^2 - \frac{V_0^2}{R_L} T_3 \quad (41)$$

or

$$V''_R = \sqrt{\frac{L_2 I_2^2}{C_1} - \frac{2V_0^2 T_3}{C_1 R_L}} \quad (42)$$

It should be emphasized that the output ripple is less than the sum of the values obtained from equations (40) and (42) since the peak variations of each occur at different times during the cycle. Equation (40) shows that the output ripple V'_R is directly proportional to the capacitor impedance and verifies why capacitors with low dissipation factors are desirable. Equation (42) verifies that large capacitance and small inductance values as well as high frequency operation are desirable in reducing the output ripple.

For most applications, capacitors are presently available which will maintain the output ripple below 0.1 volt peak to peak without additional filtering. As an example, electrolytic capacitors with a 1200 microfarad and 50-volt dc rating at 2 percent maximum dissipation factor are available in a package size of 12.3 cm³.

Additional filtering may be included as required.

IV. OUTPUT OVERLOAD PROTECTION

Many applications require the voltage regulator to limit the input power to a specified value as well as not damage the regulator during output short circuit or overload conditions.

The single-ended regulator design can accomplish these requirements easily by not allowing Q1 (Fig. 2) to conduct until the transformer has been completely discharged (time $T_2 - T_1$). By the addition of a single winding on the transformer, a signal generated during the transformer discharge time can be used to prohibit the control section from driving transistor Q1 on until all of the transformer stored energy has been expended. The voltage induced into this sense winding is given by:

$$V_3 = \frac{N_3}{N_2} (V_0 + V_{CR1}) \quad (43)$$

From equation (43) the minimum sense voltage will occur during an output short circuit condition

($V_0 = 0$) and can be controlled to the desired value by proper selection of N_3 . Note that this feature not only allows for protection during a short circuit condition but also during any overload condition.

From equation (32), the input power is proportional to the transistor duty cycle T_1/T_3 . The duty cycle will decrease during an overload condition since the transformer discharge time (from equation (25)) is inversely proportional to the secondary voltage. Therefore, an output overload condition will actually result in a decrease in the input power.

Incorporating this minor addition to the circuit provides for a reliable overload protection as well as a reduction in the input power during an overload condition.

V. SINGLE-ENDED SWITCHING TRANSFORMER REGULATOR

The output voltage of the single-ended switching transformer dc-to-dc converter of Figure 2 can be precisely regulated by controlling the operating frequency and/or duty cycle of transistor Q1. Since many acceptable techniques exist for providing transistor Q1 with the desired signal, the control section will not be discussed in detail but will be mentioned briefly to stress some of the more important considerations in designing this section.

Figure 5 is a typical block diagram of the complete switching regulator that has been used exten-

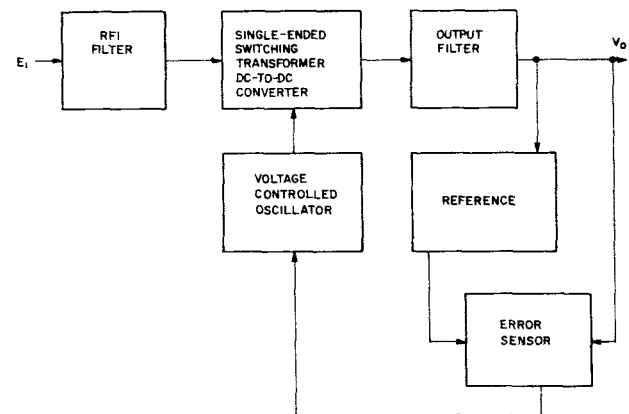


FIGURE 5. BLOCK DIAGRAM OF SINGLE-ENDED SWITCHING TRANSFORMER DC-TO-DC REGULATOR

sively in designing reliable, efficient, compact regulators for a variety of applications. The input voltage E_1 is connected to the input RFI filter. The output of the filter is connected to the input of the single-ended dc-to-dc converter (Fig. 2) which converts the input voltage to an electrically isolated output voltage. The output voltage is filtered and compared to the reference voltage. The difference is amplified and then provides a signal to the voltage controlled oscillator (VCO). The output of the VCO is a square wave and drives the single-ended dc-to-dc converter at the required frequency to maintain the desired output voltage. The output of the VCO is connected to the single-ended dc-to-dc converter through a pulse transformer to maintain the required electrical isolation between the input and output voltages.

For applications where the input voltage remains relatively constant, it is normally desirable to drive transistor Q1 (Fig. 2) into saturation for a fixed peak current each cycle. If the input voltage is variable, it is sometimes advantageous to drive Q1 on for a period of time T_1 , which is inversely proportional to the input voltage E_1 . This enables Q1 to operate at a fixed peak current each cycle regardless of the input voltage and provides the maximum power available from the regulator at the minimum input voltage.

VI. PRINCIPAL ADVANTAGES

The single-ended switching transformer regulator offers many distinct advantages as compared to conventional methods of regulation. Some of the principal features are discussed in the following paragraph.

One of the major current transient conditions in the push-pull method of conversion, as discussed previously, is caused by the inability to properly match the transistors' switching characteristics. The single-ended switching regulator, requiring only one transistor, eliminates this problem completely.

The single-ended technique eliminates the possibility of transformer saturation, a major cause of current transients in the push-pull version.

Unlike the push-pull converter, both primary and secondary voltage and current peak values can be precisely controlled to the desired levels by the proper selection of circuit parameters. This feature will allow the transistor to operate at a controlled stress level and will result in a significant improvement in reliability.

With only one power stage required (Fig. 2), a precisely regulated voltage, electrically isolated from the input power source, can be obtained. Conventional methods normally require two or more stages and significantly more components.

Since the voltage induced in the transformer windings is proportional to the number of turns in each winding, multiple output voltages are possible by proper selection of the transformer secondary windings.

This regulator is capable of a one cycle response time.

Overload protection can be incorporated by the addition of a transformer winding used to ensure the complete discharge of the transformer prior to turning on Q1 (Fig. 2). Note that the input power will be reduced during an output overload condition.

The maximum output power per regulator can be determined by equation (39). If additional power is required, direct paralleling of the outputs of two or more stages can be accomplished without affecting the regulator performance. These stages may use either a common or separate control section.

Another feature of the single-ended switching transformer regulator is that less-complicated RFI filters are required. This is possible because current waveforms are essentially constant from unit to unit.

Since transistor power losses during switching times (ON and OFF) are normally much less than the losses in the push-pull converter, the single-ended switching regulator can be operated at relatively high frequencies. A reduction in size and weight, plus an improvement in efficiency, will normally be realized by using this single-ended design.

VII. FUTURE EFFORTS

From equation (39), the maximum output power for a specific application (E_1 is constant) is dependent on the transistor switching capabilities (I_1 and V_{CE}) and the regulator efficiency (η). By selecting a family of transistors capable of delivering various output power levels, "standard" modules can be designed. Direct paralleling of these modules for increased output power could be accomplished as required. The only design necessary would consist of selecting the proper number of secondary turns N_2 where

$$N_2 = \frac{N_1 (V_0 + V_{CR1})}{V_{CE} - E_1} \quad (44)$$

and one resistor value in the control section to obtain the desired output voltage.

To further reduce the regulator size and weight as well as to improve the reliability, recent efforts have been directed toward designing a standard integrated circuit control section that could be used for practically all applications. At present, it appears to be both possible and feasible to develop the complete control section in one package, with the exception of two "test select" resistors — one to adjust time T_1 (Fig. 2) and the other to adjust the output voltage to the desired level. This will result in a further size reduction as compared to the present design.

APPENDIX DESIGN PROCEDURE

The following procedure is included to provide a systematic approach that may be used in designing the single-ended switching transformer regulator. No attempt is made to specify components or component stress levels to be used since reliability requirements vary with the application.

Sufficient time is allowed for the transformer to transfer all of the stored energy prior to switching on the transistor. This operating condition normally results in improved efficiency and less radio frequency interference with a sacrifice in the total output power capability of the regulator. In the event additional output power is required, direct paralleling of the output of two or more regulators is recommended.

In selecting the transistor in step 1, it should be noted that the maximum output power is limited by the peak collector current I_1 and the collector to emitter voltage V_{CE} (equation (39)).

The efficiency η in step 2 is dependent on several factors including the input voltage, switching frequency, transformer wire size, and components, and can be determined accurately only by thorough analysis. Provided state-of-the-art components are used and the operating frequency is nominal for the components used, an efficiency of 0.9 should normally be attainable, provided the forward voltage drop across diode CR1 is much less than the output voltage V_0 .

1. Select the transistor to be used and determine the collector to emitter voltage V_{CE} that the transistor is capable of reliably blocking and substitute into equation (45):

$$\frac{T_2}{T_1} = \frac{V_{CE}}{V_{CE} - E_1} \quad (45)$$

Solve for the ratio $\frac{T_2}{T_1}$.

2. Determine the maximum output power (P_O) desired and substitute the value into equation (46).

$$I_1 = \frac{2P_O}{\eta E_1} \frac{T_2}{T_1} \quad (46)$$

Solve for I_1 .

Provided the transistor selected in step 1 cannot reliably switch the peak collector current I_1 calculated in equation (46), it is necessary to select a transistor with increased I_1 and or V_{CE} capability and repeat steps 1 and 2.

3. Determine the transformer turns ratio N_1/N_2 from equation (47).

$$\frac{N_1}{N_2} = \frac{V_{CE} - E_1}{V_0 + V_{CR1}} \quad (47)$$

4. Select the desired transistor on time T_1 and determine the transformer primary inductance from equation (48).

$$L_1 = \frac{E_1 T_1}{I_1} \quad (48)$$

5. From the transformer design manual, determine the transformer core type and size, and the number of secondary turns required (step 3 determines the ratio of primary and secondary turns N_1/N_2). Care should be taken to ensure that the inductance remains relatively constant over the operating range.

6. Select diode CR1 with the following characteristics:

(a) Minimum reverse breakdown voltage

$$V_r = \frac{N_2}{N_1} E_1 + V_0 \quad (49)$$

(b) Capability to switch the peak forward current I_2 where

$$I_2 = \frac{N_1}{N_2} I_1 \quad (50)$$

- (c) Capability to conduct a current which decreases linearly from I_2 (from step b) to 0 in time $T_2 - T_1$ where

$$T_2 - T_1 = \frac{N_2 E_1 T_1}{N_1 (V_0 + V_{CR1})} \quad (51)$$

at a diode duty cycle given by

$$\frac{T_2 - T_1}{T_2} = \frac{E_1 N_2}{E_1 N_2 + N_1 (V_0 + V_{CR1})} \quad (52)$$

7. When a low output voltage ripple is required, a capacitor should be selected with as low a dissipation factor and as high a capacitance value as necessary.

The following equations are included as a guide in determining the capacitor type and capacitance value required.

The ripple caused by the capacitor impedance is given by

$$V'_R = (I_2 - \frac{V_0}{Z_L}) (Z_c) \quad (53)$$

The ripple produced by the transfer of the energy from the transformer to the capacitor is given by

$$V''_R = \sqrt{\frac{L_2 I_2^2}{C_1} - \frac{2 V_0^2 T_3}{C_1 R_L}} \quad (54)$$

Additional output filtering may be included when required.

N66 32612

ELECTRICAL POWER SYSTEMS STUDIES AT MSFC

By

Edward E. Dungan

SUMMARY

Electrical power systems applicable to earth orbital and to lunar surface missions are discussed. Saturn Instrument Unit lifetime extensions will require fuel cells and/or radioisotopes for primary power. Lunar surface vehicles such as the Mobile Laboratory (MOLAB) will use fuel cells that must be optimized for mass savings. Two computer programs are discussed and one is described.

I. INTRODUCTION

Electrical power systems studies in progress at MSFC include those applicable to both earth orbital and lunar surface missions. Current Saturn Instrument Units obtain primary power from onboard batteries that are capable of about six hours of continuous operation in the one to five kilowatt range. Missions requiring several days to a few weeks will depend upon fuel cells for primary electrical power. Extended missions, several weeks to one year, will necessarily be dependent upon radioisotopes for continuous primary electrical power since both battery and fuel cell masses would become prohibitive. Fuel cells and radioisotopes are both attractive for lunar surface missions. Solar devices are not being considered at this time since the long lunar night would require excessive storage batteries.

In advanced systems studies it is important that terminology be clearly defined to avoid confusion. The word "system" in this paper is defined to include one or more of the following: a primary power supply, a secondary power supply, an auxiliary power supply, a power distribution subsystem, and a heat dissipator such as a radiator. Radioisotopes, fuel cells, or batteries are used as primary power supplies depending upon the mission considered. Secondary power supplies, usually rechargeable batteries, also take care of short term peak loads. Auxiliary power supplies are used in low power applications for extended periods; for example, systems for nuclear auxiliary power (SNAP).

II. INSTRUMENT UNIT RADIOISOTOPE POWER SYSTEM

The Martin Company (Baltimore), under contract NAS8-20092, is investigating the application of radioisotopes to the Saturn Instrument Unit (IU). The title of the contract is "Establishing Design and Development Criteria for a Saturn Type Instrument Unit Electrical Power System (Radioisotopes)."

A. PURPOSE AND OBJECTIVES

The purpose of the Martin study is to set forth the basis for the integration of a radioisotope power supply into an Instrument Unit, not the design and technology or the development of a nuclear power module itself. The long range objectives for application purposes are to develop, test, and check out a power system and to build a system that will be compatible with launch vehicle missions. Constant power levels of 1 to 5 kWe will be required for mission durations from 1 to 24 months for the immediate earth orbital applications.

Assumptions and guidelines for the study include the following:

1. Assume that the power supply will be versatile enough that relatively minor modifications will be required to adapt it to various missions with power levels of 1 to 5 kWe and mission durations of 1 to 24 months.
2. The power supply will operate efficiently in any or all environments to be encountered such as launch; ascent; and orbital, escape, lunar, or deep space trajectories.
3. The power supply will be compatible with the electrical system and the configuration of Saturn type vehicles. Radiators will be designed for location within, on, or near the IU and for non-interference with operation of IU components (such as sensors or antennas).

4. Saturn IU electrical loads will be adhered to. Peak power demands may vary up to five kWe depending upon mission requirements.

5. The preliminary design of a radioisotope power supply should seriously consider the modular concept where, for example, generators of one kWe may be used in modules of one to five units. The complications of radiation shielding, including biological, should be anticipated in mass-tradeoff and design studies.

6. Availability of isotopes will be considered in detail and the selection of such isotopes will be made, with NASA's approval, by the contractor in the initial contract phase.

7. Associated nuclear radiation hazard problems of handling, launch, flight, and reentry will be studied and solutions satisfactory to all cognizant government agencies will be suggested during the early phases of the development program.

8. Reliability will be paramount and a testing program will be anticipated that will verify power supply reliability under all operating constraints. Minimum mass will be of major importance but will not be dominant over reliability.

B. STATUS AND SCHEDULE

The contract was initiated in July 1965. The first phase will be completed in March 1966. Four tasks are included in this phase: Task 1, Preliminary Evaluation; Tasks 2 and 3, Conceptual Design and Vehicle Integration; and Task 4, Data and Reports.

C. PROGRAM PLANS

Initial findings indicate the desirability of designing 500 W (net electrical) thermoelectric modules and limiting continuous IU power to 2 kWe. About 90 percent of the available lower Lunar Excursion Module (LEM) adapter surface is used for heat rejection radiators when low thermoelectric cold junction temperatures are desired. The module housing structure associated with Saturn integration will require additional design definition as system load specifications are established. The influence of the frontal generator fuel loading concept on the excess heat dump mechanism is to be studied.

The objectives of the next phase include the development and laboratory testing of a thermoelectric radioisotope power supply employing electrical heaters to simulate the isotope heat input. The simulator will meet all the design criteria and guidelines given above. The scope will include the design and

development of the instrumentation required to monitor the simulator's performance. Operating manuals will include a description of the power supply, operating procedures, operational limits, and preliminary performance data. An experimental program plan will be developed for each laboratory test.

III. LUNAR SURFACE VEHICLE POWER SYSTEM

Electrical power system studies were completed during 1965 for lunar roving vehicle applications. Two vehicle design contracts that included fuel cells as the primary power supplies were completed by Boeing Company (NAS8-11411) and Bendix Systems Division (NAS8-11287). These studies were constrained for the Mobile Laboratory (MOLAB) mission manned operation of 14 days on the lunar surface in a shirtsleeve environment. Power profiles varied substantially throughout the mission because of electrical wheel drive loads over rough terrain. Reactant consumption rates were found to be sensitive to fuel cell design characteristics; thus, substantial mass penalties would be incurred if the system was not optimized. Computer programs were developed and used as a tool in power system preliminary design. Boeing's program is given here as an example of design application.

A. MOLAB FUEL CELL OPTIMIZATION PROGRAM

The selected mission required total power loads of five to six kWe. Power and energy logic is shown in Figure 1. These requirements were applied to a computer program that optimized payload mass.

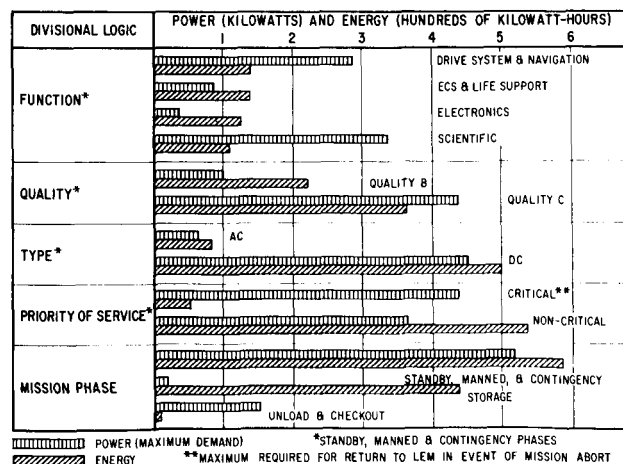


FIGURE 1. POWER AND ENERGY

Minimum mass constraints included the following:

1. Load profile
2. Radiator specific cooling capacity as a function of time
3. Maximum radiator area constraint
4. Voltage regulation constraint
5. Candidate fuel cell characteristics.

The results of the computer calculations included the following:

1. Relative mass comparison of fuel cell candidates
2. Startup time and parasitic energy requirements
3. Mass penalty as a function of specified voltage
4. Mass penalty as a function of varying power profiles.

A flow diagram that describes the program's capabilities is shown in Figure 2. The quality parameters are mission oriented and not part of an

analytical optimization. The program served as a very useful tool in reducing mass requirements in Boeing's preliminary design studies.

B. IN-HOUSE COMPUTER PROGRAM

A joint study with in-house MSFC contractor personnel was made on an electrical power system for MOLAB (Appendix A). The primary purpose of the study was to develop parameters for an in-house computer program to be used in the analysis of the various mission constraints for lunar power applications. The power profile is shown in Appendix B. The computer program is described in Appendix C.

IV. CONCLUSIONS

Space power systems for extended missions usually represent a substantial percentage of the total payload mass. It becomes imperative that computer optimization techniques, such as those described in this paper, be applied in the program definition phase preceding design and development. Technology development may also benefit in considering the results of these applications. Mission requirement projections for future technology developments may not always predict optimum parameters, but basic classes of applications can be defined.

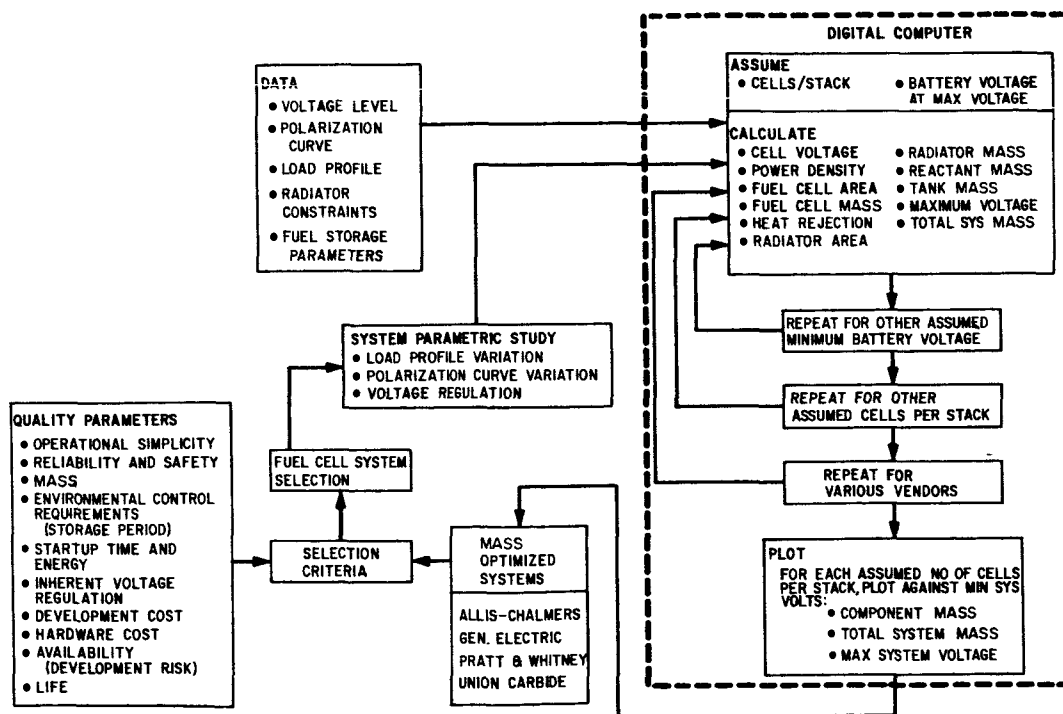


FIGURE 2. FUEL CELL SELECTION AND ANALYSIS

APPENDIX A

MOLAB STUDY ANALYSIS

A. SUMMARY

A study analysis was performed on the electric power system for the Lunar Mobile Laboratory (MOLAB) [1].

The primary chemical electric power system (CHEPS) consists of hydrogen/oxygen gas fuel cell modules, support reactant storage tankage, and a heat rejection mechanism in the form of a radiator. The secondary power system consists of a battery charged by an isotope power source. The functions of monitoring and control are provided by the power distribution system (PDS). The areas for investigation are as follows:

1. The interrelationships between arbitrary system parameters for a typical constant load profile and optimum system mass are determined for CHEPS.
2. The effects upon optimum CHEPS mass under load profile variations or arbitrary system parameters are examined.
3. A functional block diagram of the PDS is synthesized.
4. PDS equipment requirements are related to environment and internal functions.
5. Power areas within the PDS and interface are defined.

The study of item 1 showed that results obtained from "exact" and "linearized" closed voltage/current plots in the range of interest for hydrogen/oxygen fuel cells are invariable. Under the assumptions and conditions investigated, a broad minimum is found surrounding a specific system mass of 0.92 kg/kWh.

Findings relating to item 2 indicate a weak relationship between the number of fuel cells and the overall specific system mass for the profile investigated. Specific system mass varies from 0.77 kg/kWh for 7 fuel cell modules, each of 900 watt capacity, to 0.81 kg/kWh for 11 fuel cell modules, each of 900 watt capacity. Net difference in mass is 45.5 kg.

A block diagram of the PDS, as related to item 3, indicates the necessity of load separation into areas requiring good regulation and those where regulation is less important. Each area mentioned is serviced by a separate fuel cell bank. An additional fuel cell bank supplies loads which are intermittent but which require good regulation through power conditioning equipment. A diode switching arrangement, free of transient generation, is used to buffer fuel cell banks connected to intermittent loads.

Equipment requirements, as related to item 4, were examined relative to vibration, shock, acceleration, temperature, humidity, corrosive atmosphere, radiation, and combined effects. Certain environmental hazards such as electrical interference and dumped waste in vacuum are indicated. Equipment will be compatible with launch pad environment, Apollo launch, and six month lunar storage, as well as terrestrial transportation.

The major area of interest in item 5 was finding the proper mix of manual and automatic controls. Findings indicated a requirement for completely automatic control with a fail-safe stipulation. Failure of automatic control will cause a reversion to a manual override mode. A further stipulation requires that failure during the automatic mode will not damage interfacing equipment.

B. INTRODUCTION

The CHEPS for the MOLAB comprises a large fraction of total vehicle mass. It is significant that activity be directed analytically, for management of vehicular mass, in the area of CHEPS mass optimization. This report does not attempt to make specific recommendations for a particular design concept, nor does it attempt to compare or deduce basic fuel cell concepts. These aspects have been well covered in previous reports [2,3]. This study seeks to further investigate selected topics of the analytical relationships existing between the electric power system and the established 14-day mission sequence [4]. Full utilization of computer programming techniques has been employed to accomplish these objectives.

The PDS performs the task of total power management and control in the electric power system;

although it is a minor fraction of system mass, its relationship to system performance and reliability is large. Selected functional aspects of the PDS are therefore a topic of this report.

C. OPERATIONAL-SEQUENCE-ORIENTED POWER PROFILE

1. General

Mass optimization of hydrogen/oxygen fuel cell electric power systems depends upon accurate assessments not only of total energy requirements, but also of power levels and durations. These considerations result directly from the variations in fuel cell efficiency with the level of power demand.

The establishment of a detailed operational sequence [4] permits development of an electric power demand profile, consequentially related to the operations described elsewhere in this report (Table A-I and Appendix B).

2. Guidelines and Assumptions

For the purpose of analysis of the specific mission power demand on the primary fuel cell electric power system and the related mass optimization, several guidelines and assumptions follow:

a. Integrated power demands related only to communication, navigation, telemetry, life support, locomotion, and astronaut entry and exit are presented.

b. Loads related to hole drilling, scientific measurements, etc., are not considered.

c. Loads related to launch operational checkout are exempt as it is assumed that cryogenic topping occurs after checkout but before launch.

d. Loads related to post LEM truck landing and roll-off phase and checkout are exempt; it is assumed that such operations are executed either under battery power or that potential fuel cell demands are negligible.

e. Power expenditures related to the dormant phase are derived from battery banks supported by nuclear electric power supplies.

f. No provision is made for contingencies not named above or related to the operational sequence.

3. Analysis

Each hour of the operational sequence [4] makes new demands on the electric power system. As each function is performed, an integrated running total is summated and is subtotaled for the particular day. Table A-I and Appendix B are a numerical and graphical accounting of these demands.

Because of the large variation from initial to final airlock pumping power, the demands are shown as simple spikes of momentary duration. Each spike denotes the entry or exit of the astronaut and consumes 0.1 kWh. During driving sequences, starting with the tenth day, power is increased because of requirements for driving illumination during the lunar darkness. It is assumed that cabin illumination is extinguished to conserve fuel during sleeping hours and during periods of absence from the vehicle.

The 14-day average power level is about 3.0 kWe. The daily average demand is 70.5 kWh per 24 hour day.

TABLE A-I
SUMMARY OF DAILY POWER REQUIREMENTS

Day	kWh
1	68
2	65
3	73
4	67
5	78
6	81
7	58
8	90
9	73
10	79
11	64
12	88
13	58
14	46
TOTAL	988

D. PRIMARY ELECTRIC POWER SYSTEM MASS OPTIMIZATION

1. General

For the purposes of analysis, the primary MOLAB power system is considered to consist of:

- a. Hydrogen/oxygen fuel cell modules for generation of primary electric power.
- b. Storage tankage for cryogenic storage of hydrogen and oxygen.
- c. A heat rejection mechanism in the form of a space radiator.

The secondary power system, consisting of the battery banks, supplies the power required for start-up and is charged by a nuclear electric power source during all phases after launch. The heat generated by the nuclear power source is not a consideration, as it is assumed that such heat (about 1200 W) will be used for equipment temperature conditioning during the dormant phase and will contain its own radiator for excess heat dissipation.

2. Linearized Mass Optimization at Constant Load

A computer program that optimizes system mass under a constant load for arbitrary parameters is given in Appendix C. A linear approximation of the voltage/current curve was used. A sample run is included with numerical results. Optimization is accomplished for a mission duration of 336 hours. The current efficiency, first thought to be an arbitrary parameter, has proved to be a constant determined by atomic constants. The exact value is more nearly 0.0113 rather than the 0.015 kg per ampere hour that was used in the example. Results given in the main body of this report used the more accurate constant [5]. For the arbitrary parameter shown, optimum specific mass is shown to occur at a loading of 21 amperes and to have a value of 0.914 kg/kWh. The word "cell" as used in the appendix actually refers to a 900 W Allis-Chalmers fuel cell module. Voltage/current curves are taken from Reference 6. Specific mass varies in an extremely weak manner in the region of optimum loading.

3. Exact Mass Optimization at Constant Load

A computer program was again synthesized for optimization of system mass for constant load. The difference between this program and the one described in Section 2 is that a 100-point matrix of voltage and current points was taken from Reference 6. The results for specific system mass did not differ by more than one part in ten thousand from the findings of Section 2 in the vicinity of optimum loading. The results are invariable between linear and exact analysis.

4. Mass Optimization Related to Variable Load Profile

A third computer program was developed for mass optimization under variable load profile. A minimum for specific system mass was not found for these parameters.

5. Mass Optimization Related to Load Profile Variation

All values of load profile related to the referenced operational sequence and given in Appendix B were varied in 10 percent increments and run through the program developed in Section 4. The accurate value of 0.0113 kg per ampere hour was used for this analysis.

Table A-II is an accounting of various wattage levels by hours used as input data in the analysis and varies in 10 percent increments from nominal.

TABLE A-II
KILOWATT LEVELS FOR PROFILE VARIATIONS

Hours	-30%	-20%	-10%	Nom.	+10%	+20%	+30%
17.00	4.72	5.40	6.07	6.75	7.43	8.10	8.78
0.50	4.62	5.28	5.94	6.60	7.26	7.92	8.58
38.50	4.37	5.00	5.62	6.25	6.88	7.50	8.13
4.00	4.20	4.80	5.40	6.00	6.60	7.20	7.80
0.50	3.92	4.48	5.04	5.60	6.16	6.72	7.28
27.75	1.98	2.27	2.56	2.85	3.14	3.42	3.71
2.50	1.82	2.08	2.34	2.60	2.86	3.12	3.38
114.75	1.58	1.80	2.02	2.25	2.48	2.70	2.93
125.00	1.40	1.60	1.80	2.00	2.20	2.40	2.60

E. POWER DISTRIBUTION SYSTEM (PDS)

1. General

The MOLAB PDS interfaces with each subsystem requiring current within the MOLAB vehicle as well as all of the generators of electric power and storage battery banks. The primary function of the PDS is to monitor, control, and regulate all expenditures of electrical power. Placed in this position, between source and load, the PDS must budget individual subsystem power requirements and arbitrate individual demands as related to proper total system function. This area is most critical when related to total system performance and reliability.

2. Command Functions

A generalized functional block diagram is shown in Figure A-1. Note that the philosophy de-

veloped above is applicable to the relationship of PDS between source and load. Remote command and remote display are defined as signal functions received or transmitted by command receivers or transmitters which may be aboard MOLAB. Actual

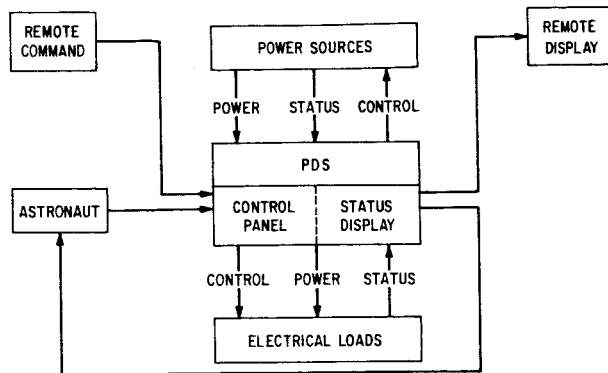


FIGURE A-1. POWER DISTRIBUTION SYSTEM FUNCTIONAL INTERFACE BLOCK DIAGRAM

origin and destination of such control functions may be at the blockhouse, Deep Space Instrumentation Facility, or LEM as related to prelaunch or postlaunch checkout. Possible requirements related to signal coding, source identification, or anti-jamming are not considered part of the PDS function and are beyond the scope of this report. Power-demand control for command receivers is not a PDS function during the dormant phase. All MOLAB operational responses are available upon receipt of applicable remote commands.

Local command functions received by the PDS originate in the sources of power, electrical equipment loads, and the astronauts. These command functions elicit automatic responses, depending upon their mutual relationship, or normalcy, and may be manually inhibited or actuated by the astronaut.

3. General Requirements and Problem Areas

The level of astronaut activity, established in the previously referenced 14-day operational sequence, firmly precludes from consideration any but the highest level of automaticity in the PDS. Out-of-tolerance function is proclaimed by both visible and audible signal, as such a condition may arise while the astronauts sleep.

Failure of any single element of the PDS will not lead to degradation of performance or loss of function. A malfunction detection system will be incorporated

to perform self-check operations upon the decision logic section. Full use will be made of widely available, compact, highly reliable integrated circuits and multiple redundancy voting logic in both these areas.

Load division will be such that intermittent loads such as air conditioning, locomotion, air lock pumping, etc., which may not require good regulation, are bus separated from loads such as navigation, communication, etc., where better regulation may be required. Load separation, along with the accepted requirements for fuel cells, of voltage variation limited to 28 ± 2 V for a three-to-one change in load should preclude all necessity of prime power regulating devices of questionable reliability and performance. However, if instrument circuits are voltage sensitive, line isolation and regulation should be provided locally within the equipment involved.

A buffering arrangement can be used as a means of isolating intermittent load transients (Fig. A-2). Power diodes of large junction areas are connected between fuel cell modules. Application of intermittent loads back-biases the diode and affords a smooth load transition such that the more constant load bus

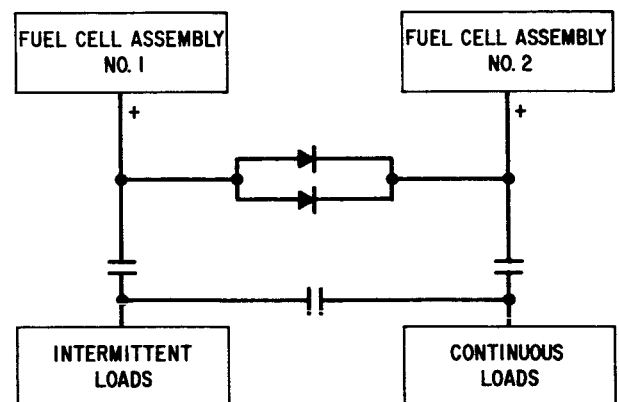


FIGURE A-2. KILOWATT LEVELS FOR PROFILE VARIATIONS

undergoes a slight decrease in voltage, whereas the voltage on the intermittent bus drops and is isolated. Since power diodes are small, compact, and may be structure mounted and paralleled, with potential drops not exceeding 1 volt and 100 amperes or more, no heat dissipation or regulation problem is encountered.

Incorporation of automatic control, if improperly attempted, can result in a degradation of reliability in the event of a failure. The same is true for a malfunction detection system. Failure of an auto-

matic control or malfunction detection system will cause the system to revert to the manual override mode. Such failure, furthermore, must not damage interfacing equipment.

4. Environmental Considerations

All externally located connective wiring, clamps, etc., must withstand the combined effects of vacuum, ultraviolet radiation, and lunar temperature extremes. Further requirements are to withstand the shock and vibration associated with Apollo launch, LEM truck landing, and terrestrial transportation. All major components will be sealed and shielded from RFI and be immune to the effects of humidity or dumped wastes in vacuum.

F. RESULTS

Several tentative results can be drawn from the analysis of previous sections.

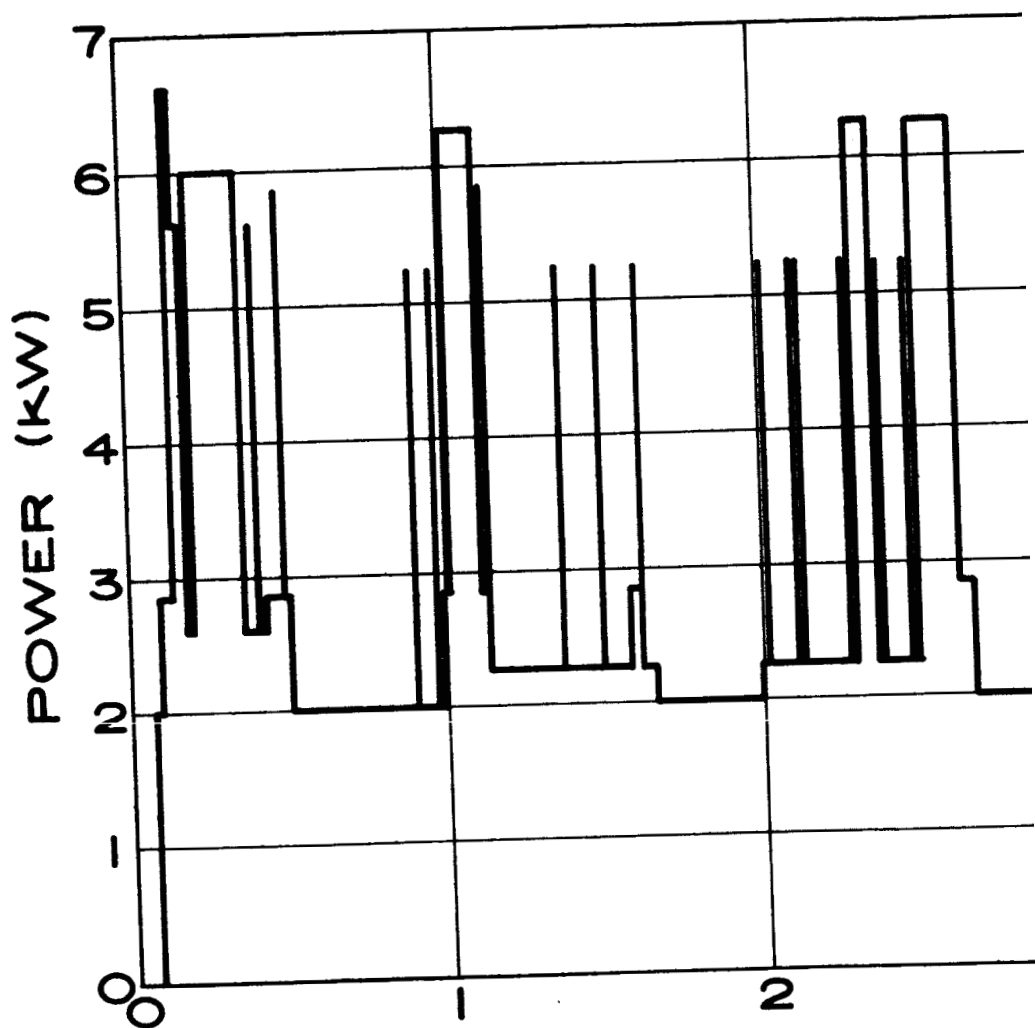
1. A variable load profile rather than a constant load profile is necessary for accurate optimization of system mass.

2. Small variations in variable load profile produce small variations in specific system mass.

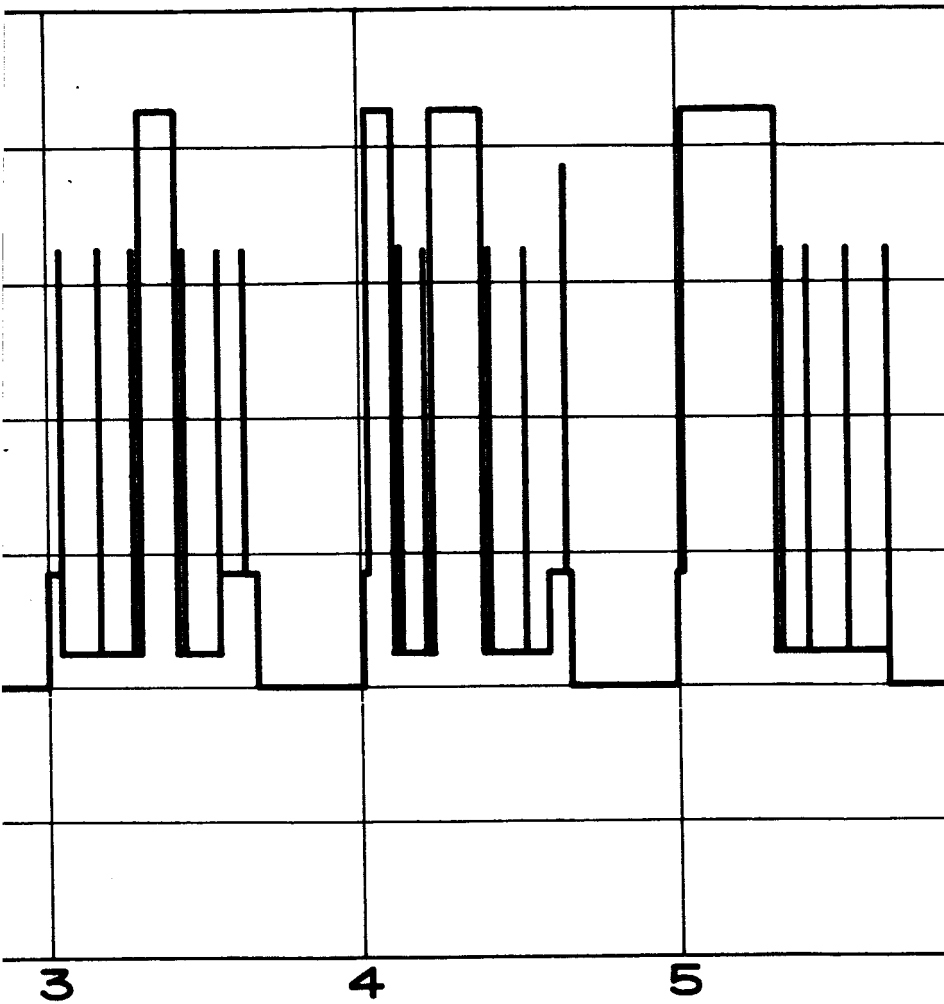
3. The power distribution system, although it represents only a small fraction of power system mass, will play a large role in system performance and reliability.

4. The power distribution system should be fully automated and fail safe, returning to the manual override mode under failure.

5. Load division should be maintained between intermittent and continuous loads.

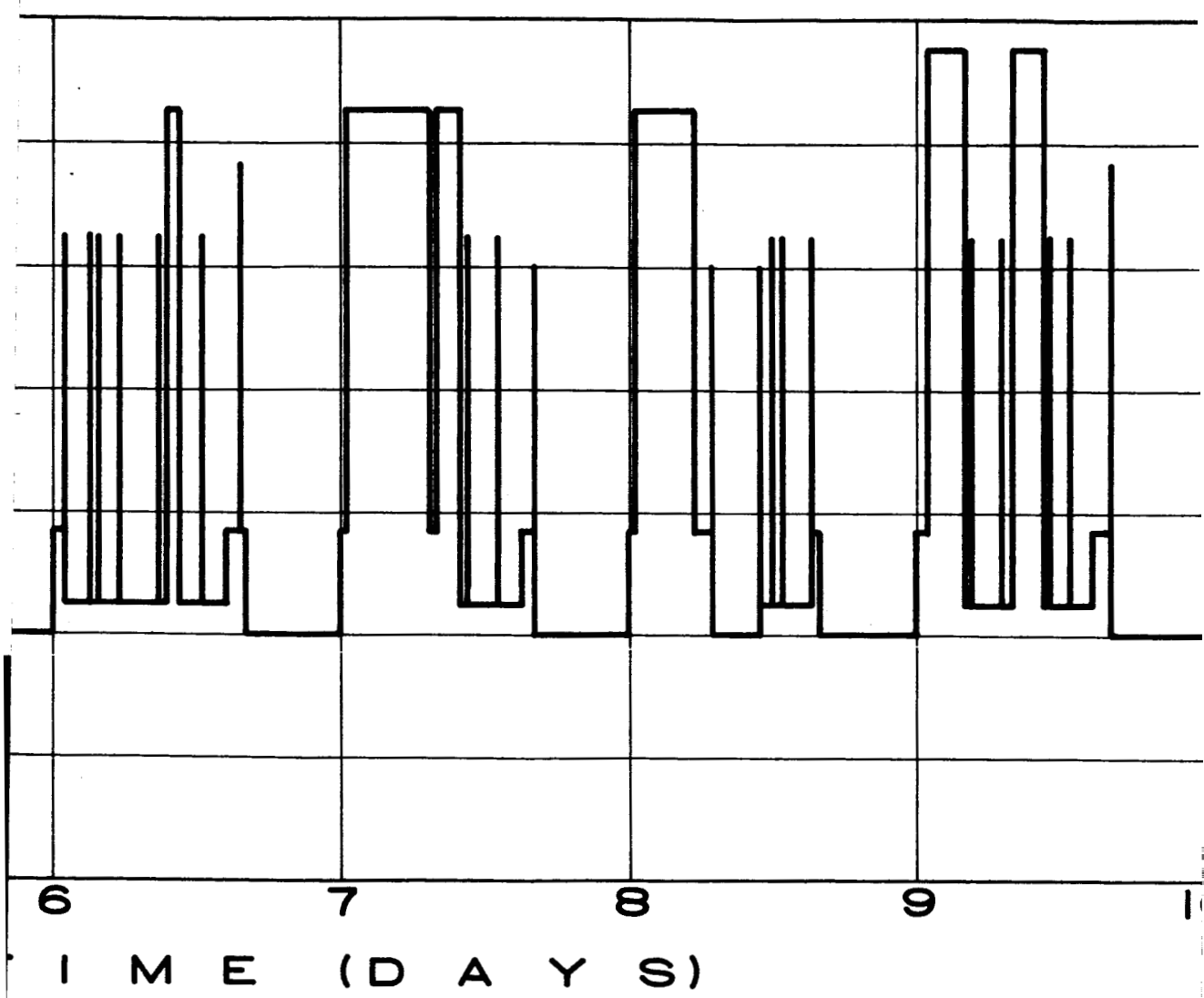


39-1



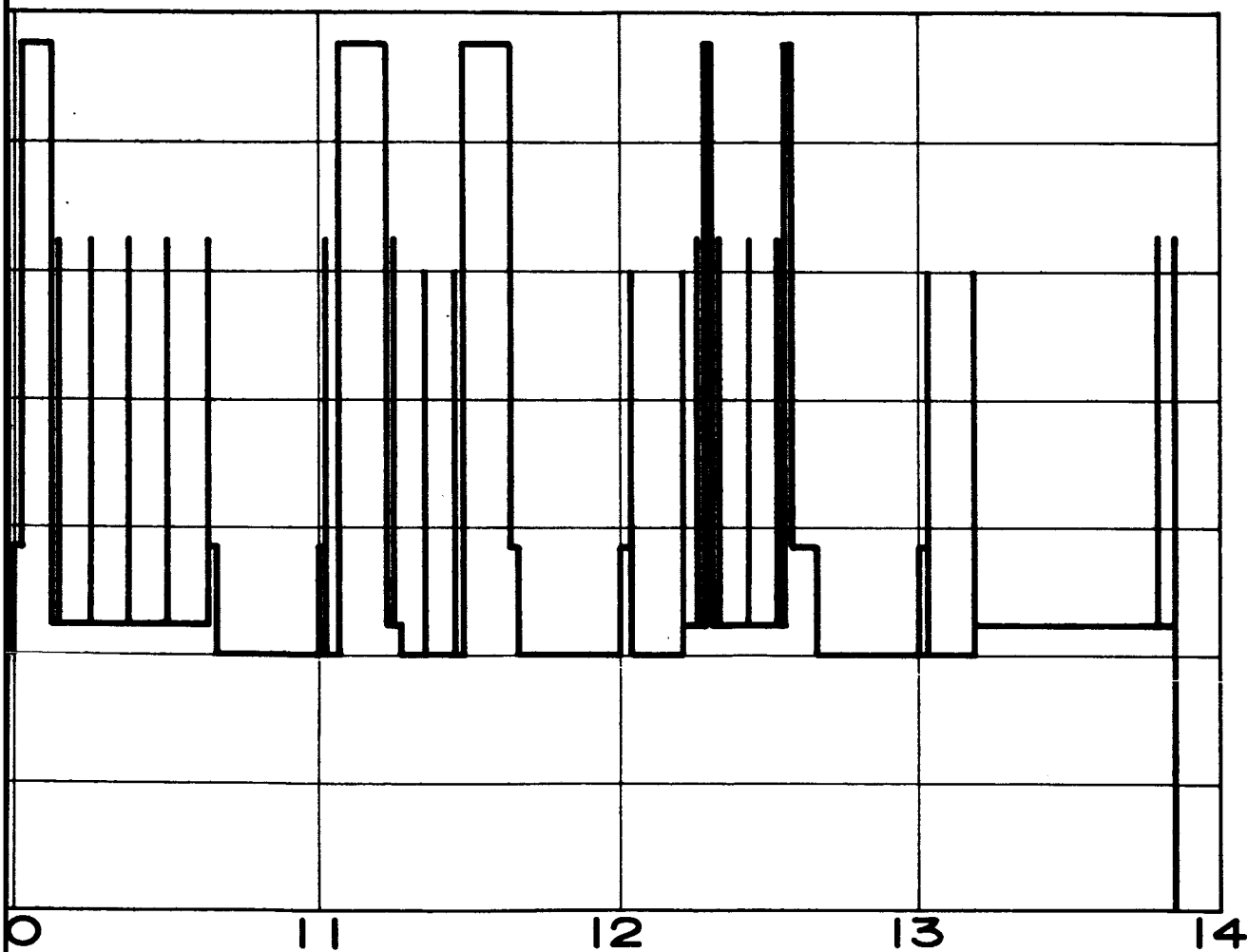
T

39-2



~~3~~ 40-1

APPENDIX B

MOLAB ELECTRICAL POWER SYSTEM LOAD DEMANDS RELATED TO
14-DAY OPERATIONAL SEQUENCE

40-2

53

APPENDIX C

COMPUTER PROGRAMS FOR FUEL CELL MASS OPTIMIZATION

A. STATEMENT OF PROBLEMS

The efficiency of a fuel cell is highest at light loads and the specific fuel consumption is lowest. To operate a fuel cell at light loads requires an oversize, and hence heavier, fuel cell. For a given mission profile and duration there is a design that has a minimum overall mass including fuel cells, fuel, tankage, and heat radiator. Two types of optimization would be useful for system design: first, an optimization of system mass at constant load for missions of arbitrary duration; second, a program that could optimize the design for a specific load profile.

B. SUMMARY OF WORK DONE

Three computer programs were written, debugged, and run successfully. These are:

1. Constant load mass optimization for arbitrary fuel cell parameters as follows: ratio of tank mass to fuel mass, mass of fuel cell, radiator mass in kilograms per watt, fuel mass in kilograms per ampere hour, fuel cell open circuit voltage, fuel cell internal resistance, fuel cell maximum efficiency, and total operating time at constant load. The values of open circuit voltage and internal resistance were chosen to closely follow the nonlinear EI curve of the fuel cell in the region of interest.

2. As above but with an exact rather than a linearized EI characteristic for the fuel cell. The optimums obtained with both programs were identical, justifying the simplicity of the linearized analysis. The cell EI curve was put in as a matrix of one hundred numbers (voltages) at one-ampere increments of fuel cell current taken from curves supplied by the manufacturer.

3. A load profile analysis and mass optimization were written and run to accept up to 20 successive steps of arbitrary duration in the load profile and pertinent fuel cell data. This gives as an output, the voltage regulation, fuel, and other masses and net kilograms per kWh for the mission as a function of the number of fuel cells used.

C. CONSTANT LOAD MASS OPTIMIZATION PROGRAM

Assumptions:

1. Tank mass is a constant factor, A, times total fuel mass.
2. Fuel consumption is a constant factor, D, times total ampere hours.
3. Radiator mass is a constant factor, C, times radiated thermal power in watts.
4. The fuel cell mass is a constant, B, in kilograms.
5. The fuel cell efficiency at light load is U.
6. All power not delivered to the load is delivered to the radiator.

Procedure:

The fuel cell is run in 1-ampere increments up to the maximum number of amperes allowed for a prescribed mission duration of T hours. The total fuel consumption, electrical output, heat output, and radiator, tankage, and fuel mass are computed. The net-mass-to-kWh ratio is computed for each operating level and printed in the results. Visual inspection of the computed answers quickly shows the optimum operating point from the standpoint of minimum net kilograms to kWh as well as the range of loads over which the mass does not deviate from the minimum by a prescribed tolerance.

Mathematical Analysis:

1. Amperes, X, is an independent variable.
2. XT is total ampere hours where T is operating time.
3. DX is total fuel mass.
4. ADX is total tank mass.
5. E is the open circuit fuel cell voltage, R is the resistance; hence E- $\frac{X}{R}$ is the output voltage.

6. $(E - XR)$ times X is P , the output power, in watts.

7. $0.001 PT$ is the output kWh.

8. $\frac{EX}{U}$ is the theoretical input power.

9. $\frac{EX}{U} - P$ is thermal power to radiator.

10. $C \left(\frac{EX}{U} - P \right)$ is the radiator mass.

11. $B + (1 + A) DXT + C \left(\frac{EX}{U} - P \right)$ is net system mass.

12. Mass-to-kWh ratios are obtained by dividing line 11 by line 7.

D. EXACT CONSTANT LOAD MASS OPTIMIZATION PROGRAM

This program is identical with the previous program except that the voltages at one ampere increments are $E(1)$ for zero amperes on open circuit voltage; $E(2)$ is the output voltage at 1 ampere, etc., up to $E(100)$, the output voltage at 99 amperes.

Mathematical Analysis:

The only differences from program I are the respective steps:

6. $XE (K - 1)$, where X is K , the output power.

7. $TXE (K - 1) (0.001)$ is the output kWh.

8. $\frac{E(1) X}{U}$ is the input power.

9. $\frac{E(1) X}{U} - XE (K - 1)$ is the power to the radiator.

10. Radiator mass is C times Step 9.

11. $B + (1 + A) DXT + C \frac{E(1) X}{U} - XE (K - 1)$ is net system mass.

E. EXACT LOAD PROFILE MASS ANALYSIS PROGRAM

In addition to mass, this program computes voltage regulation for each step of the profile and interpolates on the input EI matrix to determine the exact voltage and current for a specified profile power. Complete parameters are generated for system designs employing any desired total number of fuel cells, including fractional, and for fuel cells of any characteristics as in the programs described in C and D.

Input Data:

In addition to input data on the fuel cell, the following is set into the data cards: the minimum and the maximum number of fuel cells that are to be used; the number of intermediate designs that are to be analyzed; and the fuel cell load profile in successive T_i , P_i (where P_i is the power level of a particular step in the load profile and T_i is its duration). All steps of constant power level may be grouped together if desired to minimize input data.

Procedure:

1. As a first step the total kWh is computed by integrating the power profile. During this integration, the maximum power level is noted.

2. Next, a system having the minimum number of cells is analyzed. For this system the maximum watts per cell and the current per cell are computed from the input power, the thermal power, and the radiator mass. The radiator is sized to the maximum watts computed in step one by multiplying the waste-power-per-cell times the number of cells.

3. Each step of the profile is next considered. From the power level per cell, the corresponding voltage and current are obtained by quadratic interpolation.

4. From the current per cell times the number of cells, the total ampere hours and fuel for the particular cell are integrated.

5. After integration of the last step, total fuel consumption and tank mass are obtained.

6. The steps from 2 to 5 are then repeated for another assumed number of fuel cells.

Mathematical Analysis:

Little novelty in mathematical analysis arises except in the greater logical complexity and from the fact that voltage and current must be interpolated

between the matrix values to obtain prescribed output power. Because power is not linear in voltage and current, the interpolation involves the solution of a quadratic equation. The interpolation is otherwise linear.

REFERENCES

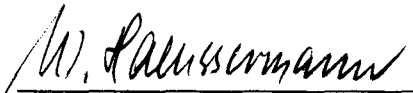
1. Delong, C. O.: ALSS MOLAB Studies, Section 10, Task Report on Power System Studies, TMX-53032. 10, Marshall Space Flight Center, October 27, 1964.
2. Dungan, E. E.; and Delong, C. O.: Apollo Logistic Support Systems MOLAB Studies, Fuel Cell Power Systems for MOLAB, IN-R-ASTR-64-13, Marshall Space Flight Center, March 16, 1964.
3. Merrifield, D. V.: MOLAB Power System Considerations. Future Studies Branch, John F. Kennedy Space Center, May 25, 1964.
4. King, R. L.; and Meyers, O. R.: Apollo Logistic Support Systems MOLAB Studies, Task Report on Mission Operational Aspects Study. TMX-53032. 2, Marshall Space Flight Center, March 1964.
5. Platner, J. L.; and Hess, P. D.: Static Moisture Removal Concept for Hydrogen-Oxygen Fuel Capillary Fuel Cell. Allis-Chalmers Research Division, September 1963.
6. Hydrogen-Oxygen Fuel Cell Systems for Space Applications. Space and Defense Sciences Department, Allis-Chalmers Research Division, August 1963.

APPROVAL

RESEARCH ACHIEVEMENTS REVIEW NO. 7, SERIES 14

The information in these reports has been reviewed for security classification. Review of any information concerning Department of Defense or Atomic Energy Commission programs has been made by the MSFC Security Classification Officer. These reports, in their entirety, have been determined to be unclassified.

These reports have also been reviewed and approved for technical accuracy.

A handwritten signature in cursive script, appearing to read 'W. Haussermann', is written over a horizontal line.

W. HAEUSSERMANN

Director, Astrionics Laboratory

DISTRIBUTION

MSFC INTERNAL

DIR	1
DEP-T	1
DEP-A	1
AST-P	1
CC	1
CC-P	1
LR	1
MA-S	1
PA	2
E-DIR	6
F&D-CH	1
R-DIR	3
R-S	1
R-TS	1
R-AS	5
R-AERO (Through Branch Level)	30
R-AERO-T	9
R-ASTR	25
R-RP-R (Reserve)	50
R-COMP (Through Branch Level)	10
R-COMP-T	5
R-ME (Through Branch Level)	21
R-RP (Through Branch Level)	8
R-P&VE (Through Branch Level)	79
R-QUAL (Through Branch Level)	26
R-QUAL-T	8
R-TEST (Through Branch Level)	12

DISTRIBUTION (continued)

MSFC INTERNAL (Cont')

LVO	2
I-DIR	1
I-I/IB-MGR (Through Branch Level)	10
I-V-MGR (Through Branch Level)	10
I-E-MGR	3
I-MICH-MGR	20
I-MT-MGR	2
MS-T	25
MS-IP	2
MS-IL	8
MS-I, Daniel Wise	1
Air Force Space Systems Division Huntsville, Alabama	1

NASA HEADQUARTERS

Dr. Mac C. Adams, Code R, Washington, D. C.	1
Mr. Milton B. Ames, Jr., Code RV, Washington, D. C.	1
Mr. Walter Beckwith, Code MTP, Washington, D. C.	1
Dr. Raymond L. Bisplinghoff, Code A, Washington, D. C.	1
Mr. Edmond C. Buckley, Code T, Washington, D. C.	1
Mr. Oliver Bumgardner, Code MLT, Washington, D. C.	1
Mr. Roland H. Chase, Code RET, Washington, D. C.	1
Mr. Fred J. DeMeritte, Code RV-1, Washington, D. C.	1
Mr. Robert W. Dunning, Code RBA, Washington, D. C.	1
Dr. James B. Edson, Code R-1, Washington, D. C.	1
Mr. Albert J. Evans, Code RA, Washington, D. C.	1
Mr. Harold B. Finger, Code RN, Washington, D. C.	1
Mr. W. Foster, Code SM, Washington, D. C.	1
Mr. Robert Freitag, Code MC, Washington, D. C.	1
Mr. Edward Z. Gray, Code MT, Washington, D. C.	1
Dr. John Holloway, Code SC, Washington, D. C.	1
Maj. Gen. David M. Jones, Code MD-P, Washington, D. C.	1
Dr. Walton L. Jones, Code RB, Washington, D. C.	1
Dr. Hermann H. Kurzweg, Code RR, Washington, D. C.	1
Mr. William E. Lilly, Code MP, Washington, D. C.	1
Dr. Douglas R. Lord, Code MTS, Washington, D. C.	1
Mr. Ivan Mason, Code MAT, Washington, D. C.	1
Dr. George E. Mueller, Code M, Washington, D. C.	1

DISTRIBUTION (continued)

NASA HEADQUARTERS (Cont')

Mr. Joseph L. Murphy, Code KR, Washington, D. C.	1
Mr. Boyd C. Myers, Code RD, Washington, D. C.	1
Dr. J. Naugle, Code SG, Washington, D. C.	1
Dr. Homer E. Newell, Code S, Washington, D. C.	1
Mr. E. O. Pearson, Jr., Code RV-1, Washington, D. C.	1
Maj. Gen. Samuel C. Phillips, Code MA, Washington, D. C.	1
Mr. Maurice J. Rappersperger, Code MTE, Washington, D. C.	1
Mr. Melvin G. Rosche, Code RV-2, Washington, D. C.	1
Mr. Charles T. D'Aiutolo, Code RV-1, Washington, D. C.	1
Mr. J. Warren Keller, Code RV-1, Washington, D. C.	1
Mr. J. L. Sloop, Code RC, Washington, D. C.	1
Mr. S. M. Smolensky, Code MCD, Washington, D. C.	1
Mr. Frank J. Sullivan, Code RE, Washington, D. C.	1
Mr. William B. Taylor, Code MT, Washington, D. C.	1
Dr. M. Tepper, Code SF, Washington, D. C.	1
Mr. Adelbert Tischler, Code RP, Washington, D. C.	1
Mr. Theofolus Tsacoumis, Code RET, Washington, D. C.	1
Mr. Gene A. Vacca, Code REI, Washington, D. C.	1
Dr. John M. Walker, Code RET, Washington, D. C.	1

CENTERS

Mr. H. Julian Allen, Director NASA, Ames Research Center Moffett Field, California 94035	2
Dr. Kurt H. Debus, Director NASA, John F. Kennedy Space Center Kennedy Space Center, Florida 32899	2
Mr. Paul F. Bikle, Director NASA, Flight Research Center P. O. Box 273 Edwards, California 93523	2
Dr. John Clark, Acting Director NASA, Goddard Space Flight Center Greenbelt, Maryland 20771	1
Dr. William H. Pickering, Director NASA, Jet Propulsion Laboratory 4800 Oak Grove Drive Pasadena, California 91103	2
Dr. Floyd L. Thompson, Director NASA, Langley Research Center Langley Station Hampton, Virginia 23365	2

CENTERS (Cont')

Dr. Abe Silverstein, Director NASA, Lewis Research Center 21000 Brookpark Road Cleveland, Ohio 44135	2
Mr. Warren Gillespie Code EA 5 NASA, Manned Spacecraft Center Houston, Texas 77001	15
Mr. J. P. Claybourne, EDV-4 Chief, Future Studies Office NASA, John F. Kennedy Space Center Kennedy Space Center, Florida 32899	1
Dr. Winston E. Kock NASA, Electronics Research Center 575 Technology Square Cambridge, Massachusetts 02139	2
Mr. A. R. Lawrence Management Analysis NASA, Electronics Research Center 575 Technology Square Cambridge, Massachusetts 02139	25
Mr. John Boyd, Technical Assistant Office of Assistant Director for Astronautics NASA, Ames Research Center Moffett Field, California 94035	1
Mr. Chesley H. Looney, Jr., Ass't Chief Advanced Development Division NASA, Goddard Space Flight Center Greenbelt, Maryland 20771	1
Mr. James F. Connors, Chief Office of Research Plans and Programs NASA, Lewis Research Center 21000 Brookpark Road Cleveland, Ohio 44135	1
Mr. James E. Calkins Office of Research and Advanced Development NASA, Jet Propulsion Laboratory 4800 Oak Grove Drive Pasadena, California 91103	1
Mr. A. R. Raffaelli PR-2 NASA, John F. Kennedy Space Center Kennedy Space Center, Florida 32899	1

DISTRIBUTION (continued)

CENTERS (Cont')

Dr. A. H. Knothe Code TEC NASA, John F. Kennedy Space Center Kennedy Space Center, Florida 32899	1
Mr. Robert Hinckley NASA, Electronics Research Center Room 323 B 575 Main Street Cambridge, Massachusetts 02139	1
Dr. William G. Melbourne Mail Stop 180-300 Jet Propulsion Laboratory 4800 Oak Grove Drive Pasadena, California 91103	1
Scientific and Technical Information Facility Attn: NASA Rep. (S-AK/RKT) P. O. Box 33 College Park, Maryland 20740	25
Mr. H. M. Drake, Chief Advanced Planning Office NASA, Flight Research Center Edwards Air Force Base Edwards, California 93523	1

DEPARTMENT OF DEFENSE

Dr. William W. Carter Chief Scientist U. S. Army Missile Command Bldg. 5250 Redstone Arsenal, Alabama	1
Mr. John McDaniel Technical Director Research and Development Directorate U. S. Army Missile Command Bldg. 4505 Redstone Arsenal, Alabama	12
Lt. M. V. Vasilik Arnold Air Force Base Tullahoma, Tennessee 37389	30

CONTRACTORS

The Boeing Company Attn: Mr. John Pehrson Huntsville Industrial Center Huntsville, Alabama	5
Brown Engineering Company, Inc. Mail Stop 5 300 Sparkman Drive, NW Huntsville, Alabama	5
Chrysler Corporation Attention: Mr. Howard Blood 1312 Meridian, North Huntsville, Alabama	5
Douglas Aircraft Holiday Office Center Huntsville, Alabama	5
General Electric Company Holiday Office Center Huntsville, Alabama	5
Mr. Robert A. Hardesty General Electric Company Ordnance Department 100 Plastics Avenue Room 1040 Pittsfield, Massachusetts 01201	5
Hayes International Corporation 204 Oakwood Avenue, NE Huntsville, Alabama	5
IBM Corporation 150 Sparkman Drive, NW Huntsville, Alabama	5
Lockheed Aircraft Corporation Holiday Office Center Huntsville, Alabama	5
North American Aviation, Inc. Holiday Office Center Huntsville, Alabama	5
Northrop Corporation Holiday Office Center Huntsville, Alabama	5
Sperry Rand Corporation 8110 Memorial Parkway, SW Huntsville, Alabama	5

DISTRIBUTION (continued)

CONTRACTORS (Cont')

Space Craft, Incorporated
8620 Memorial Parkway, SW
Huntsville, Alabama

Spaco, Incorporated
3022 University Drive, NW
Huntsville, Alabama

University of Alabama
4701 University Avenue, NW
Huntsville, Alabama

Vitro Corporation of America
Holiday Office Center
Huntsville, Alabama

Wyle Laboratories
Highway 20, West
Huntsville, Alabama

1

5

5

5

UNIVERSITIES AND COLLEGES

5

Alabama A&M College
Huntsville, Alabama

University of Alabama
Tuscaloosa, Alabama

Dr. Clyde Hull Cantrell, Director
Ralph Brown Draughon Library
Auburn University
Auburn, Alabama

University of California (UCLA)
Los Angeles, California

Carnegie Institute of Technology
Pittsburgh, Pennsylvania

Case Institute of Technology
Cleveland, Ohio

Clemson University
Clemson, South Carolina
Attn: Mr. J. W. Gourlay

1

1

4

1

1

1

1

DISTRIBUTION (continued)

UNIVERSITIES AND COLLEGES (Cont')

Mr. S. G. Nicholas Director of Engineering Research Clemson University Clemson, South Carolina	1
Columbia University New York, New York 10027	1
Librarian Columbia University Nevis Laboratories Irvington, New York 10533	1
University of Denver Denver, Colorado	1
Director's Office Denver Research Institute University of Denver Denver, Colorado	1
Department of Nuclear Engineering Sciences University of Florida Gainesville, Florida 32603	1
Mrs. J. Henley Crosland Director, Libraries Georgia Institute of Technology Atlanta, Georgia	9
University of Georgia Athens, Georgia	1
Louisiana State University Baton Rouge, Louisiana	1
Massachusetts Institute of Technology Cambridge, Massachusetts	1
University of Michigan Ann Arbor, Michigan	1
Mississippi State University State College, Mississippi	1
University of Mississippi University, Mississippi	1
University of North Carolina Chapel Hill, North Carolina	1

DISTRIBUTION (continued)

UNIVERSITIES AND COLLEGES (Cont')

Northeast Louisiana College Monroe, Louisiana	1
Ohio State University Columbus, Ohio	1
Ohio University Athens, Ohio	1
Oklahoma State University Stillwater, Oklahoma	1
University of Pittsburgh Pittsburgh, Pennsylvania	1
Princeton University Princeton, New Jersey	1
Library School of Electrical Engineering Purdue University Lafayette, Indiana	1
Rev. R. J. Henle, S. J. Vice President for Academic Matters and Research Director Saint Louis University 221 N. Grand Blvd. St. Louis, Missouri	2
Stanford University Palo Alto, California	1
Syracuse University Syracuse, New York	1
University of Tennessee Knoxville, Tennessee	1
Cushing Memorial Library Texas A&M University College Station, Texas	1
Mr. Harry E. Whitmore, Head Space Technology Division Texas A&M University College Station, Texas	2
University of Texas Austin, Texas	1

DISTRIBUTION (continued)

UNIVERSITIES AND COLLEGES (Cont')

Science Librarian Tulane University Library New Orleans, Louisiana 70118	1
The Joint University Libraries 419 - 21st Avenue, South Nashville, Tennessee	1
Science Library Vanderbilt University Box 1521, Station B Nashville, Tennessee	1
Virginia Polytechnic Institute Blacksburg, Virginia	1
Washington State Pullman, Washington	1
Mr. H. W. Hsu Associate Professor of Chemical Engineering University of Tennessee Knoxville, Tennessee 37916	1
Professor F. N. Peebles Department of Engineering Mechanics University of Tennessee Knoxville, Tennessee	1

**Multiple Pages Missing from Available
Version**

UNITS OF MEASURE

In a prepared statement presented on August 5, 1965, to the U. S. House of Representatives Science and Astronautics Committee (Chaired by George P. Miller of California), the position of the National Aeronautics and Space Administration on Units of Measure was stated by Dr. Alfred J. Eggers, Deputy Associate Administrator, Office of Advanced Research and Technology:

"In January of this year NASA directed that the international system of units should be considered the preferred system of units, and should be employed by the research centers as the primary system in all reports and publications of a technical nature, except where such use would reduce the usefulness of the report to the primary recipients. During the conversion period the use of customary units in parentheses following the SI units is permissible, but the parenthetical usage of conventional units will be discontinued as soon as it is judged that the normal users of the reports would not be particularly inconvenienced by the exclusive use of SI units."

The International System of Units (SI Units) has been adopted by the U. S. National Bureau of Standards (see NBS Technical News Bulletin, Vol. 48, No. 4, April 1964).

The International System of Units is defined in NASA SP-7012, "The International System of Units, Physical Constants, and Conversion Factors," which is available from the U. S. Government Printing Office, Washington, D. C. 20402.

SI Units are used preferentially in this series of research reports in accordance with NASA policy and following the practice of the National Bureau of Standards.